subcellular localization of HCV structural proteins in Huh-7 cells infected with an infectious HCV clone. Our data show that, in infected cells, HCV glycoprotein heterodimer is retained in the ER and the capsid protein is detected in association with lipid droplets. However, in contrast to previous reports, no other subcellular localization was found for these proteins. In addition, no colocalization was observed between the glycoprotein heterodimer and the capsid protein in HCV-infected cells. Electron microscopy analyses identified membrane alterations in infected cells; however, dense elements compatible with the size and shape of a viral particle were seldom observed in HCV-infected cells.

## MATERIALS AND METHODS

**Cell culture and HCV production.** Huh-7 human hepatoma cells (35) were grown in Dulbecco modified essential medium (Invitrogen) supplemented with 10% fetal bovine serum. The plasmid pJFH1 containing the full-length cDNA of JFH1 isolate, which belongs to subtype 2a (GenBank accession no. AB047639), has been described previously (42). To generate genomic HCV RNA, the plasmid pJFH1 was linearized at the 3′ end of the HCV cDNA by XbaI digestion. After treatment with mung bean nuclease, the linearized DNA was then purified and used as a template for in vitro transcription with the MEGAscript kit from Ambion. In vitro-transcribed RNA was delivered to cells by electroporation as described previously (25). Viral stocks were obtained by harvesting cell culture supernatants 1 week posttransfection. Secondary viral stocks of ca. $10^5$ 50% tissue culture infective doses/ml were obtained by additional amplifications on naive Huh-7 cells. Except for some electron microscopy studies, all of the experiments were done with Huh-7 cells infected with secondary viral stocks. For immunofluorescence studies, HCV-infected cells were treated with trypsin, seeded on coverslips, and grown for 3 to 4 days before processing for immunolabeling. Virus titration was performed as described previously (26) by immunostaining the cells with anti-E2 monoclonal antibody (MAb) 3/11.

**Antibodies.** Rat MAb 3/11 (19) was produced in vitro by using a MiniPerm apparatus (Heraeus) as recommended by the manufacturer. Mouse anti-E2 MAb AP33 has been previously described (7). Human anti-E1 MAb 1C4 (Innogenetics hybridoma clone IGH398) was obtained from a patient chronically infected with an HCV subtype 1b strain. This immunoglobulin G1 (IgG1) MAb has been mapped to the V3 region of E1 (amino acids 235 to 240) and has been shown to cross-react with E1 peptides from genotypes 1 to 6 (G. Maertens et al., unpublished data). Anti-capsid ACAP27 (28) and anti-NS3 (486D39) MAbs were kindly provided by J. F. Delagneau (Bio-Rad, France). Human anti-E2 MAb CBH5 (21), mouse anti-ERGIC-53 MAb (38), and anti-capsid MAb 6G7 (23) were kindly provided by S. Foung (Stanford University), H. P. Hauri (University of Basel, Basel, Switzerland) and H. B. Greenberg (Stanford University), respectively. Mouse anti-CD63 MAb TS63 (5) was a gift from E. Rubinstein (INSERM U602, Villejuif, France). Mouse anti-GM130 and anti-LAMP-1 MAbs were purchased from BD Biosciences. Rabbit antibodies to calnexin, calreticulin, and protein disulfide isomerase (PDI) were from Stressgen. Mouse anti-cytochrome *c* MAb 6H2.B4 was from Pharmingen. Guinea pig polyclonal antibody to human ADRP was purchased from Progen. Alexa 488-conjugated goat anti-rabbit, anti-mouse, anti-rat, or anti-human IgG, and isotype-specific Alexa488-conjugated goat anti-mouse IgG2a and Alexa555-conjugated goat anti-mouse IgG1 were purchased from Molecular Probes. Cy3-conjugated goat anti-mouse, anti-rat, or anti-guinea pig IgG were purchased from Jackson Immunoresearch (West Grove, PA).

**Indirect immunofluorescence microscopy.** Infected Huh-7 cells grown on 12-mm glass coverslips were fixed with 3% paraformaldehyde and then permeabilized with 0.1% Triton X-100 in phosphate-buffered saline (PBS). Both primary and secondary antibody incubations were carried out in PBS containing 10% goat serum for 30 min at room temperature. For double-label immunofluorescence with primary antibodies from different species, Cy3- and Alexa 488-conjugated secondary antibodies were used. For double-label immunofluorescence with anti-C MAb ACAP27 (IgG2a) and another mouse MAb (IgG1), isotype-specific Alexa 488-conjugated goat anti-mouse IgG2a and Alexa 555-conjugated goat anti-mouse IgG1 were used. Lipid droplets were stained with oil red O as described previously (22). Coverslips were mounted on slides by using Mowiol 4-88 (Calbiochem). Confocal microscopy was performed with an SP2 confocal laser-scanning microscope (Leica) using a ×100/1.4 numerical aperture oil immersion lens. Double-label immunofluorescence signals were sequentially collected by using single fluorescence excitation and acquisition settings to avoid crossover. Images were processed by using Adobe Photoshop software.

**Cell surface labeling.** Huh-7 cells infected by JFH1 virus or transfected with the plasmid phCMV-E1E2 (3) or phCMV-E1E2(LAL) (6), as well as control Huh-7 cells were used for cell surface labeling. Cells were incubated for 1 h on ice with the primary antibody. MAb 3/11 was used to detect E2 glycoprotein expressed at the cell surface. Experiments with a rabbit polyclonal anti-calnexin antiserum were carried out as a control for the lack of permeabilization of cell membranes. Cells were then washed three times with cold PBS, fixed with 3% paraformaldehyde. Alexa-488-conjugated goat anti-rat or rabbit secondary antibody incubation was carried out in PBS containing 10% goat serum for 30 min at room temperature.

**Endoglycosidase digestions.** Huh-7 cells infected by JFH1 virus or 393T cells transfected with the plasmid phCMV-E1E2 (3) were lysed with 0.5% Igepal CA-630 in TBS (50 mM Tris-Cl [pH 7.5], 150 mM NaCl). Cell lysates were used for immunoprecipitation with anti-E2 MAb AP33 as previously described (16). Immunoprecipitated proteins were eluted from protein-A Sepharose in 30 μl of dissociation buffer (0.5% sodium dodecyl sulfate [SDS] and 1% 2-mercaptoethanol) by boiling for 10 min. The protein samples were then divided into equal portions for digestion with either endo-β-*N*-acetylglucosaminidase H (endo H) or peptide:*N*-glycosidase F (PNGase F) and an undigested control. Digestions were carried out for 1 h at 37°C in the buffer provided by the manufacturer. Proteins were then analyzed by Western blotting.

**Western blotting.** After separation by SDS-polyacrylamide gel electrophoresis (PAGE), protein preparations were transferred to nitrocellulose membranes (Hybond-ECL; Amersham) by using a Trans-Blot apparatus (Bio-Rad) and revealed with a specific MAb, followed by the addition of goat anti-mouse or anti-rat immunoglobulin conjugated to peroxidase (Jackson Immunoresearch). The proteins of interest were revealed by enhanced chemiluminescence detection (ECL; Amersham) as recommended by the manufacturer.

**Electron microscopy.** For ultrastructural analysis, cells were fixed in 4% paraformaldehyde and 1% glutaraldehyde in 0.1 M phosphate buffer (pH 7.2) for 48 h. Cells were then washed in phosphate buffer, harvested, and postfixed with 1% osmium tetroxide for 1 h. They were then dehydrated in a graded acetone series, and cell pellets were embedded in Epon resin, which was allowed to polymerize for 24 h at 60°C. Ultrathin sections were cut on an ultramicrotome (Reichert, Heidelberg, Germany), collected on copper grids and stained with 1% uranyl acetate–1% lead citrate. The grids were then observed with a 1010 XC electron microscope (JEOL, Tokyo, Japan).

## RESULTS

**The glycoprotein heterodimer is located in the ER of HCV-infected cells.** Efficient viral replication of JFH1 isolate was obtained by amplification on naive Huh-7 cells with virus titers of ca. $10^5$ 50% tissue culture infective doses/ml. This allowed us to reinvestigate the subcellular localization of HCV structural proteins in the context of an infectious cycle. The subcellular distribution of HCV envelope glycoproteins was examined by confocal immunofluorescence microscopy. To define the intracellular localization of E1 and E2 during HCV infection, we looked for antibodies that recognize the glycoproteins of the JFH1 strain in immunofluorescence analyses. Huh-7 cells were either mock infected or infected with HCV, grown on glass coverslips, fixed with paraformaldehyde, and processed for indirect immunofluorescence with various anti-E1 or anti-E2 antibodies. A large panel of antibodies that were raised against HCV glycoproteins of genotype 1 was screened. However, only anti-E1 MAb 1C4 and anti-E2 MAbs 3/11, AP33, and CBH5 were found to specifically label HCV-infected Huh-7 cells, but not naive cells in indirect immunofluorescence. Immunoblot analysis confirmed that MAb 1C4 recognizes the glycoprotein E1 and that MAbs 3/11 and AP33 recognize the glycoprotein E2 of the JFH1 strain (Fig. 1A and data not shown).

HCV-infected cells stained with MAbs 1C4, 3/11, or AP33 displayed a pattern of specific fluorescence in a network of

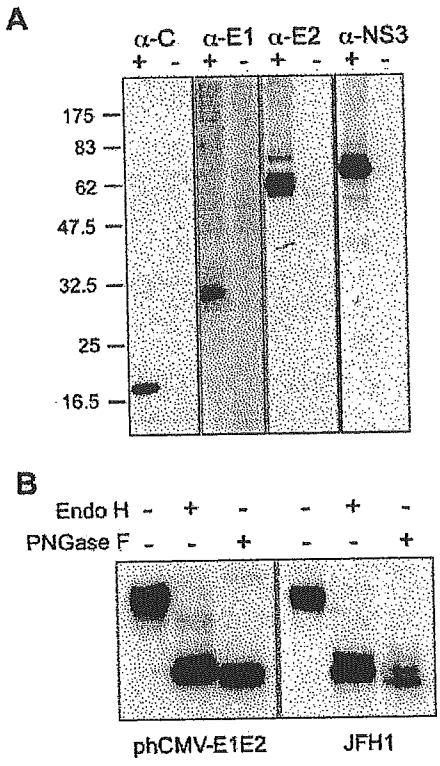


FIG. 1. Expression of HCV proteins in HCV-infected cells. (A) Analysis of the expression of HCV proteins C, E1, E2, and NS3 by Western blotting. Lysates of naive (−) or HCV-infected (+) cells were separated by SDS-PAGE and revealed by Western blotting with MAbs ACAP27 (anti-C), 1C4 (anti-E1), 3/11 (anti-E2), and 486D39 (anti-NS3). The sizes of protein molecular mass markers are indicated on the right (in kilodaltons). (B) Analyses of the glycans associated with HCV glycoprotein E2. Lysates of HCV-infected cells Huh-7 cells (JFH1) or 293T cells transfected with a plasmid expressing HCV envelope glycoproteins (phCMV-E1E2) were immunoprecipitated with anti-E2 MAb AP33. The immunoprecipitates were treated or not treated with endo H or PNGase F. Proteins were then separated by SDS-PAGE and revealed by Western blotting with the anti-E2 MAb 3/11.

cytoplasmic membranes and the nuclear envelope (Fig. 2). A very similar pattern of staining was also observed with MAb CBH5 (not shown). As expected, since they assemble as a heterodimer during their folding (11), E1 and E2 glycoproteins colocalized (Fig. 2). Interactions between E1 and E2 of JFH1 strain were confirmed by coimmunoprecipitation (data not shown). To further define the intracellular localization of HCV glycoprotein heterodimer in infected cells, double-label immunofluorescence experiments were carried out with an anti-E2 MAb. HCV-infected cells grown on glass coverslips were incubated with MAb 3/11, together with antibodies specific for various intracellular compartments. Within the secretory pathway, E2 colocalized predominantly with proteins of the ER, including calnexin (Fig. 2, calnexin), calreticulin, and PDI (not shown). In contrast to other studies (29, 37), E2 did not colocalize with the marker of the intermediate compartment ERGIC-53 (Fig. 2, ergic53) or with the Golgi marker GM130 (Fig. 2, GM130). In addition, E2 did not colocalize with markers of the endocytic pathway, such as EEA-1, a protein localized in early endosomes; CD63, a marker of multivesicular endosomes (not shown); or LAMP-1, a marker of late endosomes and lysosomes (Fig. 2, lamp-1). It is worth noting that we did not detect any change in the subcellular localization of HCV glycoprotein heterodimer when analyzed at different times posttransfection (48, 72, and 96 h) or postinfection (48 and 72 h). These findings demonstrate that the glycoprotein heterodimer localizes predominantly to the ER in HCV-infected cells, and they are in agreement with previous data obtained in the context of the expression of the full-length HCV polyprotein (17).

**The glycoprotein heterodimer is not expressed at the plasma membrane of HCV-infected cells.** Recently, it has been shown that, in some transient expression systems, a fraction of HCV envelope glycoproteins can also be detected at the plasma membrane (3, 13, 24). We therefore investigated whether HCV glycoprotein heterodimer can leave the ER and be exported to the plasma membrane in the context of HCV-infected cells.

To determine whether a fraction of HCV glycoprotein heterodimer has left the ER compartment, we analyzed whether the glycans associated with HCV glycoprotein E2 have been modified by Golgi enzymes by evaluating their sensitivity to endo H treatment. Resistance to digestion with endo H is indicative that glycoproteins have moved from the ER to at least the medial and *trans*-Golgi, where complex sugars are formed. PNGase F treatment, which removes all types of N-linked glycans, was used as a control of deglycosylation. As shown in Fig. 1B, the glycoprotein E2 remained endo H sensitive in HCV-infected cells, whereas a faint endo H-resistant band was observed for E2 expressed in cells transfected with a plasmid expressing HCV envelope glycoproteins. As previously observed (14), due to the presence of a residual *N*-acetylglucosamine at each glycosylation position after endo H treatment, the endo H-treated E2 migrated slightly more slowly than the PNGase F-treated protein. An additional slightly slower migrating band was detected for both PNGase F- and endo H-treated proteins (Fig. 1B). Such a partial resistance to PNGase F treatment has already been observed for truncated forms of HCV glycoprotein E2, as well as for E1 expressed in HCV pseudotyped particles (36).

Cell surface expression was determined by surface labeling using the anti-E2 MAb 3/11. Although an E2 staining was clearly detected in HCV-infected cells treated with Triton X-100 (Fig. 3, compare panels A and B), no E2 protein was detected at the cell surface (Fig. 3C). Interestingly, E2 was detected at the plasma membrane of Huh-7 cells transfected with a plasmid expressing HCV envelope glycoproteins of genotype 1a (Fig. 3E). It is worth noting that there was a correlation between the level of expression and cell surface detection (data not shown). In addition, as previously observed (6, 10), the level of expression of E2 at the cell surface was higher when the charged residues in the transmembrane domain of E2 were mutated (Fig. 3F). When expressed from a plasmid, the expression level of HCV envelope glycoproteins of JFH1 isolate was approximately 15 times higher than in the context of HCV-infected cells; however, they were not detected above background at the cell surface (data not shown), indicating that there might be some differences between isolates or subtypes for cell surface expression. Altogether, these data indicate that HCV glycoprotein heterodimer does not accumulate at the plasma membrane in HCV-infected cells.

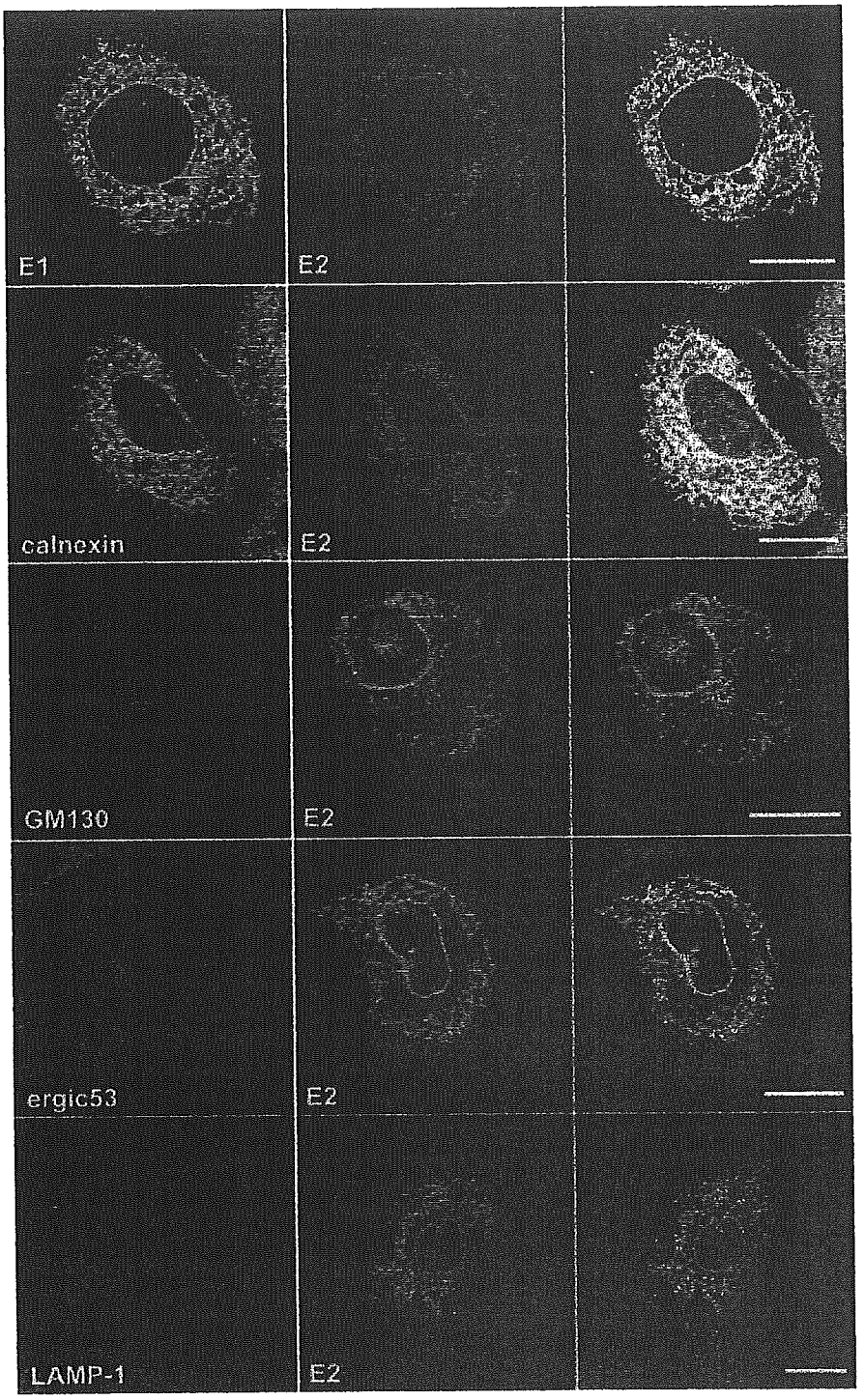


FIG. 2. Confocal immunofluorescence analysis of the intracellular distribution of HCV glycoproteins. Infected cells grown on coverslips were fixed and processed for double-label immunofluorescence for E1, E2, and the following cellular markers: calnexin, a chaperone of the ER; GM130, a Golgi matrix protein; ERGIC-53, a marker of the ER-to-Golgi intermediate compartment; or LAMP-1, a marker of late endosomes and lysosomes. Anti-E2 mouse MAb AP33 was used for the colocalization with E1. For the other experiments, E2 was revealed with the rat MAb 3/11. Representative confocal images of individual cells are shown with the merge images in the right column. Bar, 20 μm.

**Intracellular localization of the capsid protein in HCV-infected cells.** To detect the capsid protein, we used the 6G7 (23) and ACAP27 (28) antibodies, two mouse MAbs that recognize two different epitopes located at amino acids 29 to 39 and amino acids 40 to 53, respectively. Consistent with the high levels of sequence conservation among core proteins from different genotypes, both MAbs gave positive signals in Huh-7 cells infected with JFH1 virus (Fig. 4 and data not shown).

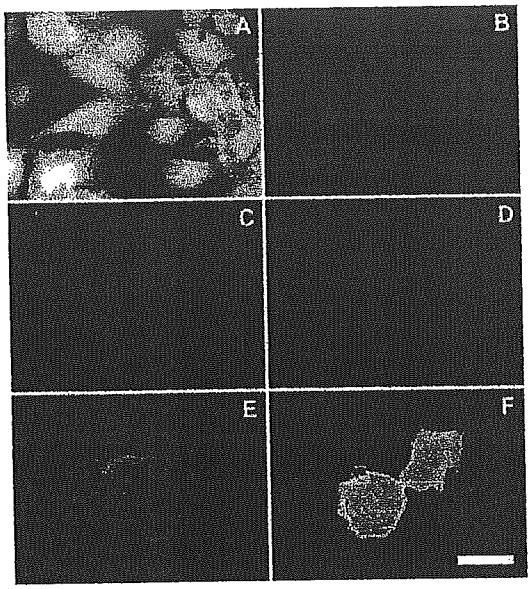


FIG. 3. Cell surface expression of HCV glycoprotein E2. Naive (B and D) or infected (A and C) Huh-7 cells grown on coverslips were labeled with the anti-E2 MAb 3/11. A set of cells was fixed with 3% paraformaldehyde and processed for immunofluorescence labeling after permeabilization with Triton X-100 (A and B). Cell surface labeling (C, D, E, and F) was carried out on ice with MAb 3/11 before the fixation with 3% paraformaldehyde and the incubation with Alexa488-labeled secondary antibody. Huh-7 cells transfected with a plasmid expressing wild-type HCV envelope glycoproteins (phCMV-E1E2; panel E) or HCV envelope glycoproteins containing a mutation of the charged residues in the transmembrane domain of E2 [phCMV-E1E2(LAL); panel F] were used as controls of cell surface expression of E2. All images were acquired and processed with the same settings. Bar, 50 μm.

Immunoblot analysis confirmed that they recognize the core protein of the JFH1 strain (Fig. 1 and data not shown). The capsid protein migrated as a single species with an apparent molecular mass of 21 kDa, which most likely corresponded to the processed form of the capsid protein from which the signal sequence of E1 has been removed.

HCV-infected cells incubated with either anti-C protein MAbs displayed very similar patterns of bright fluorescence strictly limited to the cell cytoplasm and frequently concentrated in the perinuclear region (Fig. 4 and data not shown). In contrast, naive Huh-7 cells were not stained, indicating the specificity of the labeling (data not shown). In the perinuclear region, the staining pattern often displayed ring-like structures (Fig. 4). Double-label immunofluorescence experiments were performed in order to define the intracellular localization of the C protein. We did not observe, in contrast to E2, any colocalization between C and markers of the ER, such as calnexin (Fig. 4), calreticulin, or PDI (data not shown). In contrast to another report analyzing the subcellular localization in a cell line inducibly expressing HCV structural proteins (29), the perinuclear area containing the C protein was not localized in the Golgi complex and did not colocalize with the marker of the intermediate compartment (Fig. 4). In addition, no colocalization was observed with markers of the endocytic pathway, such as EEA-1 or Lamp-1 (data not shown).

Expression with heterologous expression systems or in the context of a full-length HCV replicon has shown that HCV capsid protein can associate with lipid droplets (1, 22, 37). We therefore analyzed whether the C protein expressed in HCV-infected cells would colocalize with lipid droplets. When lipid droplets were labeled with oil red O, an association between the C protein and lipid droplets was clearly observable. However, in contrast to previous reports, a fraction of the C protein was not directly associated with the lipid droplets, and the pattern of labeling was consistent with this fraction of the C protein being localized in a membranous compartment that is associated with the lipid droplets (see zoomed inset in Fig. 4). It is worth noting that we did not detect any change in the subcellular localization of the C protein when analyzed at different times posttransfection (48, 72, and 96 h) or postinfection (48 and 72 h).

To confirm the association of C with lipid droplets, double-label immunofluorescence experiments were carried out with an antibody to ADRP, which is a marker of the cytosolic pool of lipid droplets. In most infected cells, C and ADRP displayed an extensive colocalization (Fig. 4). At a higher magnification, C and ADRP were often concentrated on different parts of single lipid droplet-like ring structures (Fig. 4 ADRP, inset). In addition, no competition between both proteins for the association to lipid droplets was observed, as judged by the relative levels of ADRP and C immunoreactive signals in individual cells (not shown).

It has been shown that a fraction of the C protein expressed with heterologous systems can be located in the nucleus (43). However, we did not detect such a subcellular localization in HCV-infected cells (Fig. 4). Other reports have also proposed that a fraction of the C protein could be associated with mitochondria (39) and/or an Apo-AII-positive compartment (1). However, double-label immunofluorescence experiments in HCV-infected Huh-7 cells did not confirm the colocalization of the C protein with Apo-AII or mitochondria (data not shown). The detection of the capsid protein in the nucleus or the mitochondria as observed in other reports is potentially due to protein overexpression, to saturation of fluorescence signals, or to the absence of particle formation.

Altogether, our results show that the capsid protein is localized at the surface of lipid droplets and in a membranous compartment that is associated with the lipid droplets.

**Relative intracellular localization of HCV glycoprotein heterodimer, capsid protein, and NS3.** HCV nonstructural proteins NS3 to NS5B are the viral components of HCV replication complex (2), and they have been shown to colocalize in Huh-7 cells containing a subgenomic replicon (20). In addition, due to the presence of NS4B, the expression of HCV nonstructural proteins induces the formation of a virus-induced structure designated the membranous web (18). HCV structural and nonstructural proteins have been shown to colocalize with the membranous web (18), suggesting that the replication and assembly factories might be located within the same virus-induced organelle. We therefore analyzed whether HCV glycoprotein heterodimer would colocalize with the C protein and whether the localization of structural proteins would overlap that of nonstructural proteins. We chose to use an anti-NS3 antibody to detect one of the components of the replication complex. Immunofluorescence with the anti-NS3 MAb was positive on HCV-infected cells (Fig. 5) and negative on control cells (data not shown). Immunoblot analysis confirmed that the

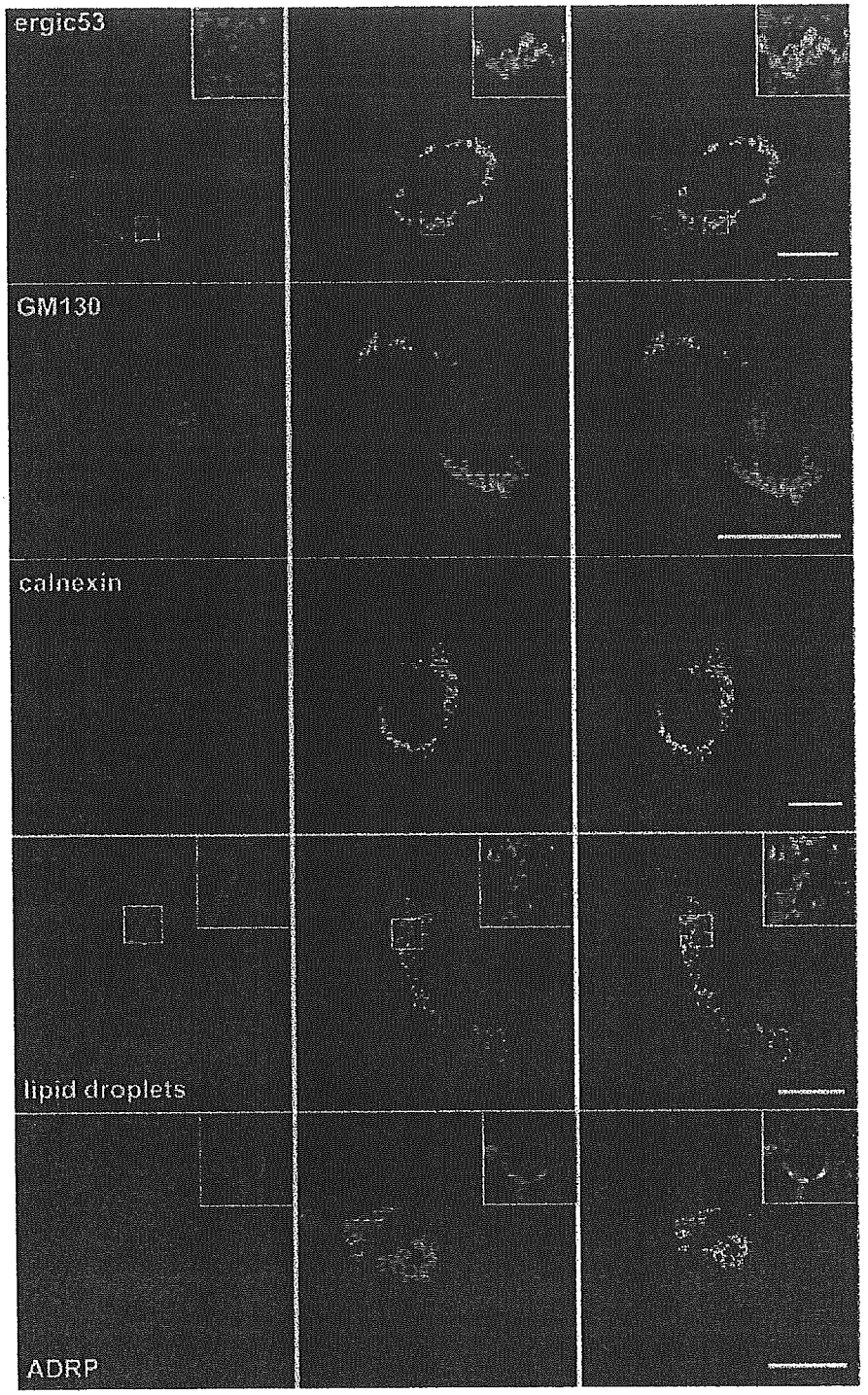


FIG. 4. Confocal immunofluorescence analysis of the intracellular distribution of the capsid protein. Infected cells grown on coverslips were fixed and processed for double-label immunofluorescence for C (green) and the following cellular markers (red): ERGIC-53, a marker or the ER-to-Golgi intermediate compartment; GM130, a Golgi matrix protein; calnexin, a chaperone of the ER; or ADRP, a marker of the cytosolic pool of lipid droplets. Lipid droplets were stained with oil red O. Representative confocal images of individual cells are shown with the merge images in the right column. Insets display zoomed views of the indicated area. Bar, 20 μm.

anti-NS3 MAb recognizes the NS3 protein of the JFH1 strain (Fig. 1A).

Double-label immunofluorescence experiments with anti-C and anti-E2 antibodies did not show any colocalization between C and E2 (Fig. 5). This is in agreement with the colocalization of E2 with ER markers and the absence of colocalization between the C protein and ER makers (Fig. 2 and 4). In contrast, a partial colocalization was observed between the

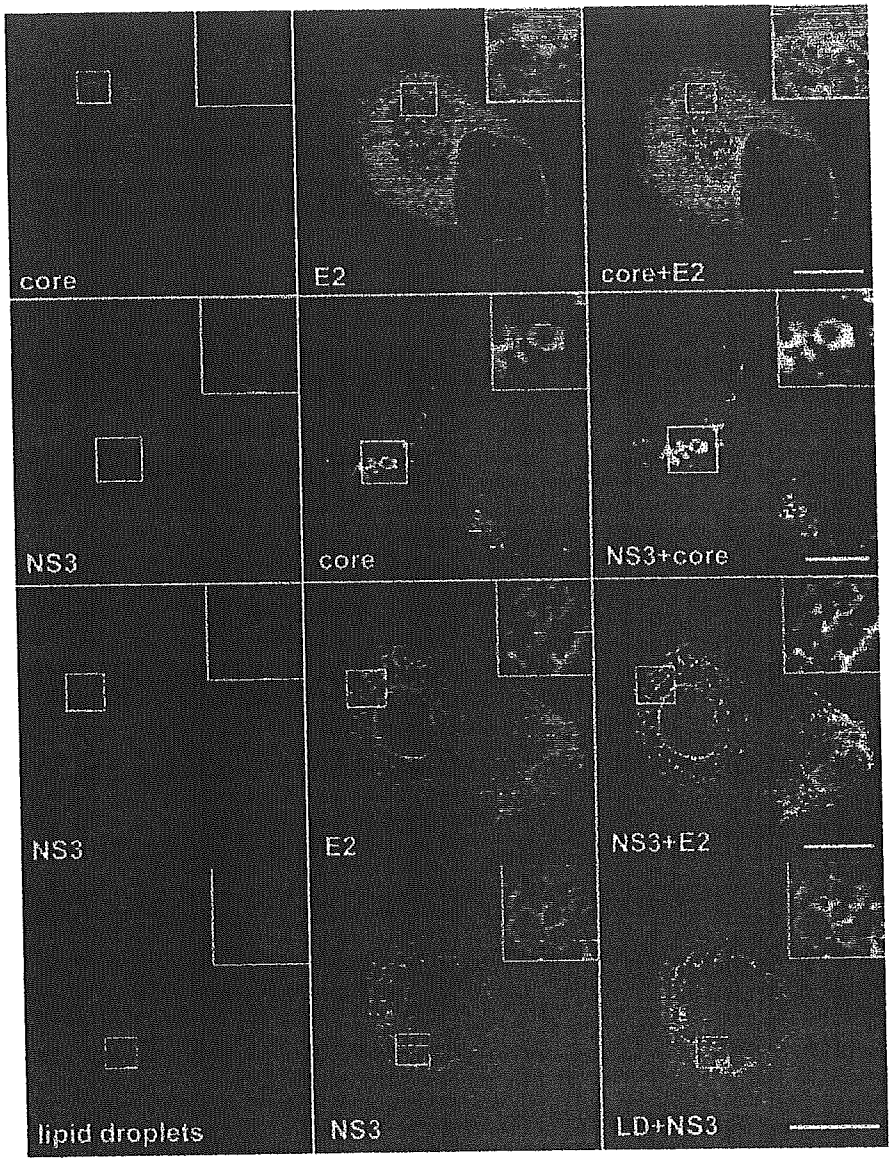


FIG. 5. Relative intracellular localization of HCV proteins C, E2, and NS3 analyzed by confocal immunofluorescence. Infected cells grown on coverslips were fixed and processed for double-label immunofluorescence for C and E2 (top row), NS3 and C (middle row), or NS3 and E2 (bottom row). Lipid droplets were stained with oil red O. Representative confocal images of individual cells are shown with the merge images in the right column. Insets display zoomed views of the indicated area. Bar, 20 μm.

C protein and NS3 and between E2 glycoprotein and NS3 (Fig. 5). NS3 displayed an ER-like pattern of immunofluorescence, which colocalized partially with E2. In addition, in a number of cells NS3 labeling was often more intense in the perinuclear area, where it partially colocalized with the C protein (Fig. 5). Interestingly, when lipid droplets were labeled with oil red O, the NS3 protein was also found around lipid droplets (Fig. 5).

**Ultrastructural aspects of HCV-infected cells.** To identify ultrastructural modifications induced by JFH1 replication and the potential presence of viral particles, we investigated Huh-7 cells containing replicative JFH1 genome by electron microscopy. In a first set of experiments, we used Huh-7 cells transfected with JFH1 genomic RNA to have virtually all of the cells containing a replicative virus (Fig. 6). We then confirmed our observations on HCV-infected cells (data not shown). Lipid droplets were often observed in cells containing replicative JFH1 genome (Fig. 6A); however, there is no evidence that lipid droplets accumulate more in HCV-infected cells than in control naive Huh-7 cells. A membranous web composed of small vesicles was also found in many Huh-7 cells containing replicative JFH1 genome (Fig. 6B) but not in naive cells (data not shown). Figure 6C shows a membranous web at higher magnification. This structure was similar to the membranous web previously identified in U-2 OS human osteosarcoma-derived cell lines inducibly expressing the HCV polyprotein and in Huh-7 cells harboring a subgenomic HCV replicon (18, 20). Virus-like particles were never found in the membranous web. Some electron-dense elements compatible in size and

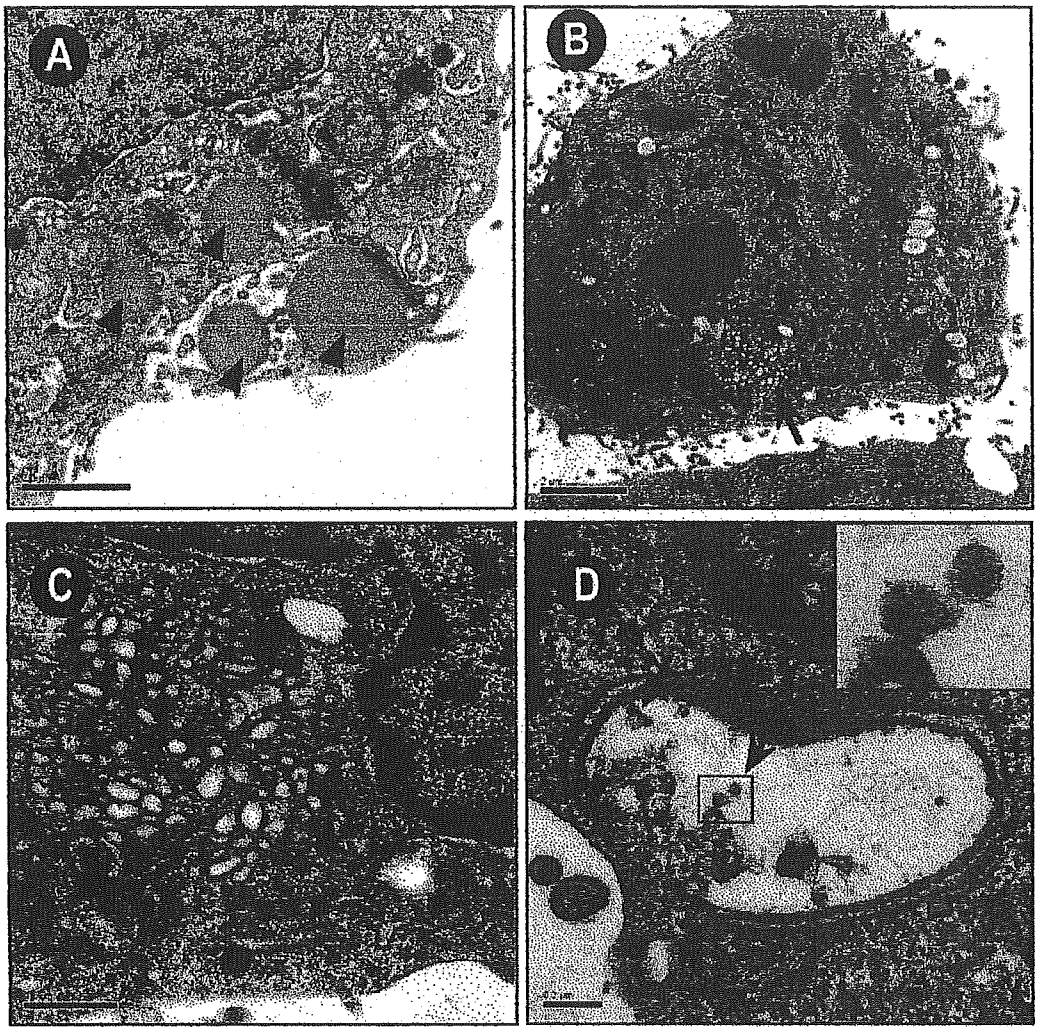


FIG. 6. Membrane alterations in Huh-7 cells containing replicative JFH1 genome visualized by electron microscopy. (A) Cell containing several lipid droplets (arrows). Bar, 2 μm. (B) Low-power overview showing a membranous web (arrow). Bar, 2 μm. (C) Higher magnification of the membranous web. Bar, 0.5 μm. (D) Small cisternae containing electron-dense elements compatible in size and shape with virus-like or core particles (arrows). Bar, 0.2 μm. Inset displays zoomed view of the indicated area.

shape with virus-like or core particles were sometimes found in small cisternae of Huh7 cells containing replicative JFH1 genome (Fig. 6D). These particles were smaller and more regular than the glycogen particles that are abundantly present in the Huh7 cells, but they were rare and their relationship with viral structures remains to be determined.

## DISCUSSION

The recent development of a cell culture model for HCV (26, 42, 44) allows the production of virus that can be efficiently propagated in cell culture. This cell culture system has allowed us to reinvestigate the subcellular localization of HCV structural proteins in the context of an infectious cycle. Here, we showed that, in infected cells, HCV glycoprotein heterodimer is retained in the ER and the capsid protein is detected in association with lipid droplets. In contrast to previous reports, the glycoprotein heterodimer and the capsid protein were not detected in other subcellular localizations. Interestingly, electron microscopy analyses identified membrane alterations in infected cells. However, dense elements compatible with viral particles were seldom observed in HCV-infected cells.

HCV glycoprotein heterodimer is retained in the ER in infected cells. This is in agreement with several studies with heterologous expression systems containing HCV envelope glycoproteins or in the context of the full-length HCV polyprotein (11, 14, 17). Indeed, ER localization signals have been identified in the transmembrane domains of E1 and E2 (8, 9). Other studies have, however, shown that a fraction of HCV envelope glycoproteins can also be found in the ERGIC and in the *cis*-Golgi apparatus (29, 37). The presence of HCV glycoprotein heterodimer in these compartments is potentially due to protein overexpression, to saturation of fluorescence signals, or to the absence of particle formation. Indeed, such localization in the ERGIC and in the *cis*-Golgi apparatus was not observed in HCV-infected cells.

HCV glycoprotein heterodimer is not exported to the plasma membrane in infected cells. In some conditions of expression, a small fraction of HCV envelope glycoproteins

has been shown to accumulate at the plasma membrane, and this led to the development of a system to pseudotype retroviral particles with HCV envelope proteins that has proven crucial for studying HCV entry (3, 13, 24, 36). However, cell surface expression of HCV glycoprotein heterodimer is not observed in HCV-infected cells, and export at the plasma membrane with the heterologous system might be due to the accumulation of small amounts of glycoproteins escaping the ER retention machinery due to saturation of this mechanism. It is worth noting that in the case of JFH1 envelope glycoproteins expressed from a plasmid, the glycoproteins were not detected at the cell surface, suggesting that there might also be some differences between isolates or subtypes for the subcellular localization of the envelope glycoproteins.

The capsid protein is detected in association with lipid droplets in infected cells. This is in agreement with other studies using heterologous expression systems or in the context of a full-length HCV replicon (1, 22, 37). However, in contrast to these studies, a fraction of the C protein was not directly associated with the lipid droplets, and this suggests a localization of the C protein in a membranous compartment that is associated with the lipid droplets, in addition to the localization of another fraction of the C protein at the surface of lipid droplets. Lipid droplets consist of a core of triglycerides and cholesterol esters surrounded by a monolayer of phospholipids and a proteinaceous coat (34). The most likely mechanism by which triglycerides and cholesterol esters end up in cytosolic lipid particles is that they first accumulate between the leaflets of the ER lipid bilayer and, after reaching a critical size, a lipid droplet would bud off the cytosolic side of the ER membrane (40). However, some droplets can remain physically connected to the ER membrane (4). From our immunolocalization study, it can be suggested that the C protein localizes at the site of lipid droplet formation. Although the C protein was not found to colocalize with the markers of ER membranes in HCV-infected cells, its localization at the potential site of lipid droplet formation suggests that the C protein does not associates with the rough ER but might attach to a subcompartment of the ER, which is potentially the smooth ER. We can also not exclude that this subcompartment corresponds to cytoplasmic raft microdomains that have been recently reported to contain the C protein (30).

The absence of colocalization between the C protein and classical markers of the ER compartment contrasts with some reports indicating that the C protein interacts with rough ER membranes (for a review, see reference 31). Interestingly, it has been reported that the traffic between rough ER membranes, the site of capsid protein synthesis, and lipid droplets is regulated by signal peptide peptidase cleavage in the C-terminal region of the capsid protein (32). It is therefore likely that in the context of HCV-infected cells, transport of the C protein to the site of lipid droplet assembly is rapid due to rapid cleavage by the signal peptide peptidase. It has also been previously reported that the different extents to which the capsid protein is associated with lipid droplets or rough ER membranes may be dependent on the amount of lipid droplets present in various cell types (22). Since HCV-infected cells accumulate lipid droplets, they provide the conditions for a shift toward accumulation of the C protein in association with lipid droplets.

The significance of the association of HCV capsid protein to a lipid droplet related compartment is not understood. Since the capsid protein is a major component of the viral particle, one might expect that this interaction plays a role in some step of virion morphogenesis. It is possible that the sites of lipid droplet formation provide a platform for nucleocapsid assembly by concentrating viral and/or cellular components that are necessary for the assembly of the nucleocapsid and/or by excluding those that inhibit this process. Interestingly, NS3 appears to partially colocalize with C in this compartment.

The glycoprotein heterodimer and the capsid protein do not colocalize in HCV-infected cells. Since the glycoprotein heterodimer and the capsid protein are the protein components of HCV particle, one would expect that these proteins would accumulate at the same site for virion assembly. Indeed, production of infectious virus particles likely requires spatially and temporally coordinated interactions of components that make up an infectious virion. The absence of colocalization between the glycoprotein heterodimer and the capsid protein would suggest that particle assembly is a two-step process involving nucleocapsid assembly, followed by a budding process occurring in two separate compartments. However, in the absence of sufficient data, it would be premature to generate a model of HCV particle assembly. To have a better idea of HCV morphogenesis, one would need to analyze the subcellular localization of HCV structural proteins in living cells. This would help elucidate the dynamics of the protein interactions between different cellular compartments.

Some viruses require membrane surfaces on which to assemble their replication complex. Such interactions have been well documented for positive-strand RNA viruses (41). In the case of HCV, a structure called membranous web has been previously identified in cell lines inducibly expressing the HCV polyprotein (18). In addition, such structures have also been shown to contain HCV RNA replication complex in cells harboring subgenomic replicons (20). Interestingly, a membranous web composed of small vesicles was also found in HCV-infected cells. However, these structures did not contain any virus-like particles, suggesting that HCV particle assembly does not occur in the membranous web.

The recent development of a cell culture model for HCV has allowed us to investigate for the first time the subcellular localization of HCV structural proteins in the context of a replicative and assembly competent virus. Interestingly, our data indicate that investigating the properties of HCV proteins expressed in heterologous systems do not necessarily reflect those that they have in the context of an infectious cycle. In conclusion, the cell culture system for HCV warrants reinvestigation of the biochemical and biological properties of HCV proteins in order to better understand their functional significance in the context of active viral replication and morphogenesis.

## ACKNOWLEDGMENTS

We thank André Pillez, Sophana Ung, and Sylvie Trassard for technical assistance. We are grateful to J. F. Delagneau, S. Foung, H. P. Hauri, H. B. Greenberg, E. Rubinstein, F. L. Cosset, and B. Bartosch for providing reagents. The data presented here were generated with the help of the Imaging Core Facility of the Calmette Campus and the Electron Microscopy Facility of the University of Tours.

This study was supported by EU grant QLRT-2001-01329 and grants from the Agence Nationale de Recherche sur le SIDA et les Hépatites Virales (ANRS) and INSERM ATC-Hépatite C. Some of the authors were supported by fellowships from the French Ministry of Research (F.H.), the ANRS (D.D. and E.B.), and the CNRS (C.V.). T.W. was partly supported by grants from the Ministry of Health, Labor, and Welfare of Japan; the Program for Promotion of Fundamental Studies in Health Sciences of the National Institute of Biomedical Innovation (NIBIO); and Research on Health Sciences focusing on Drug Innovation of the Japan Health Sciences Foundation. J.D. is an international scholar of the Howard Hughes Medical Institute.

## REFERENCES

1. **Barba, G., F. Harper, T. Harada, M. Kohara, S. Goulinet, Y. Matsuura, G. Eder, Z. Schaff, M. J. Chapman, T. Miyamura, and C. Brechot.** 1997. Hepatitis C virus core protein shows a cytoplasmic localization and associates to cellular lipid storage droplets. Proc. Natl. Acad. Sci. USA **94**:1200–1205.
2. **Bartenschlager, R., M. Frese, and T. Pietschmann.** 2004. Novel insights into hepatitis C virus replication and persistence. Adv. Virus Res. **63**:71–180.
3. **Bartosch, B., J. Dubuisson, and F. L. Cosset.** 2003. Infectious hepatitis C pseudo-particles containing functional E1E2 envelope protein complexes. J. Exp. Med. **197**:633–642.
4. **Blanchette-Mackie, E. J., N. K. Dwyer, T. Barber, R. A. Coxey, T. Takeda, C. M. Rondinone, J. L. Theodorakis, A. S. Greenberg, and C. Londos.** 1995. Perilipin is located on the surface layer of intracellular lipid droplets in adipocytes. J. Lipid. Res. **36**:1211–1226.
5. **Charrin, S., F. Le Naour, M. Oualid, M. Billard, G. Faure, S. M. Hanash, C. Boucheix, and E. Rubinstein.** 2001. The major CD9 and CD81 molecular partner: identification and characterization of the complexes. J. Biol. Chem. **276**:14329–14337.
6. **Ciczora, Y., N. Callens, C. Montpellier, B. Bartosch, F. L. Cosset, A. Op De Beeck, and J. Dubuisson.** 2005. Contribution of the charged residues of HCV glycoprotein E2 transmembrane domain to the functions of E1E2 heterodimer. J. Gen. Virol. **86**:2793–2798.
7. **Clayton, R. F., A. Owsianka, J. Aitken, S. Graham, D. Bhella, and A. H. Patel.** 2002. Analysis of antigenicity and topology of E2 glycoprotein present on recombinant hepatitis C virus-like particles. J. Virol. **76**:7672–7682.
8. **Cocquerel, L., S. Duvet, J.-C. Meunier, A. Pillez, R. Cacan, C. Wychowski, and J. Dubuisson.** 1999. The transmembrane domain of hepatitis C virus glycoprotein E1 is a signal for static retention in the endoplasmic reticulum. J. Virol. **73**:2641–2649.
9. **Cocquerel, L., J.-C. Meunier, A. Pillez, C. Wychowski, and J. Dubuisson.** 1998. A retention signal necessary and sufficient for endoplasmic reticulum localization maps to the transmembrane domain of hepatitis C virus glycoprotein E2. J. Virol. **72**:2183–2191.
10. **Cocquerel, L., C. Wychowski, F. Minner, F. Penin, and J. Dubuisson.** 2000. Charged residues in the transmembrane domains of hepatitis C virus glycoproteins play a key role in the processing, subcellular localization, and assembly of these envelope proteins. J. Virol. **74**:3623–3633.
11. **Deleersnyder, V., A. Pillez, C. Wychowski, K. Blight, J. Xu, Y. S. Hahn, C. M. Rice, and J. Dubuisson.** 1997. Formation of native hepatitis C virus glycoprotein complexes. J. Virol. **71**:697–704.
12. **De Martynoff, G., A. Venneman, and G. Maertens.** 1997. Analysis of post-translational modifications of HCV structural proteins by using the vaccinia virus expression system, p. 39–44. *In* M. Rizzetto, R. H. Purcell, and H. Gerin (ed.), Viral hepatitis and liver disease. Minerva Medica, Turin, Italy.
13. **Drummer, H. E., A. Maerz, and P. Poumbourios.** 2003. Cell surface expression of functional hepatitis C virus E1 and E2 glycoproteins. FEBS Lett. **546**:385–390.
14. **Dubuisson, J., H. H. Hsu, R. C. Cheung, H. B. Greenberg, D. G. Russell, and C. M. Rice.** 1994. Formation and intracellular localization of hepatitis C virus envelope glycoprotein complexes expressed by recombinant vaccinia and Sindbis viruses. J. Virol. **68**:6147–6160.
15. **Dubuisson, J., F. Penin, and D. Moradpour.** 2002. Interaction of hepatitis C virus proteins with host cell membranes and lipids. Trends Cell. Biol. **12**: 517–523.
16. **Dubuisson, J., and C. M. Rice.** 1996. Hepatitis C virus glycoprotein folding: disulfide bond formation and association with calnexin. J. Virol. **70**:778–786.
17. **Duvet, S., L. Cocquerel, A. Pillez, R. Cacan, A. Verbert, D. Moradpour, C. Wychowski, and J. Dubuisson.** 1998. Hepatitis C virus glycoprotein complex localization in the endoplasmic reticulum involves a determinant for retention and not retrieval. J. Biol. Chem. **273**:32088–32095.
18. **Egger, D., B. Wölk, R. Gosert, L. Bianchi, H. E. Blum, D. Moradpour, and K. Bienz.** 2002. Expression of hepatitis C virus proteins induces distinct membrane alterations including a candidate viral replication complex. J. Virol. **76**:5974–5984.
19. **Flint, M., C. Maidens, L. D. Loomis-Price, C. Shotton, J. Dubuisson, P. Monk, A. Higginbottom, S. Levy, and J. A. McKeating.** 1999. Characterization of hepatitis C virus E2 glycoprotein interaction with a putative cellular receptor, CD81. J. Virol. **73**:6235–6244.
20. **Gosert, R., D. Egger, V. Lohmann, R. Bartenschlager, H. E. Blum, K. Bienz, and D. Moradpour.** 2003. Identification of the hepatitis C virus RNA replication complex in Huh-7 cells harboring subgenomic replicons. J. Virol. **77**:5487–5492.
21. **Hadlock, K. G., R. E. Lanford, S. Perkins, J. Rowe, Q. Yang, S. Levy, P. Pileri, S. Abrignani, and S. K. Foung.** 2000. Human monoclonal antibodies that inhibit binding of hepatitis C virus E2 protein to CD81 and recognize conserved conformational epitopes. J. Virol. **74**:10407–10416.
22. **Hope, R. G., and J. McLauchlan.** 2000. Sequence motifs required for lipid droplet association and protein stability are unique to the hepatitis C virus core protein. J. Gen. Virol. **81**:1913–1925.
23. **Hsu, H. H., M. Donets, H. B. Greenberg, and S. M. Feinstone.** 1993. Characterization of hepatitis C virus structural proteins with a recombinant baculovirus expression system. Hepatology **17**:763–771.
24. **Hsu, M., J. Zhang, M. Flint, C. Logvinoff, C. Cheng-Mayer, C. M. Rice, and J. A. McKeating.** 2003. Hepatitis C virus glycoproteins mediate pH-dependent cell entry of pseudotyped retroviral particles. Proc. Natl. Acad. Sci. USA **100**:7271–7276.
25. **Kato, T., T. Date, M. Miyamoto, A. Furusaka, K. Tokushige, M. Mizokami, and T. Wakita.** 2003. Efficient replication of the genotype 2a hepatitis C virus subgenomic replicon. Gastroenterology **125**:1808–1817.
26. **Lindenbach, B. D., M. J. Evans, A. J. Syder, B. Wolk, T. L. Tellinghuisen, C. C. Liu, T. Maruyama, R. O. Hynes, D. R. Burton, J. A. McKeating, and C. M. Rice.** 2005. Complete replication of hepatitis C virus in cell culture. Science **309**:623–626.
27. **Lindenbach, B. D., and C. M. Rice.** 2001. *Flaviviridae*: the viruses and their replication, p. 991–1042. *In* D. M. Knipe and P. M. Howley (ed.), Fields virology, 4th ed. Lippincott/The Williams & Wilkins Co., Philadelphia, Pa.
28. **Maillard, P., K. Krawczynski, J. Nitkiewicz, C. Bronnert, M. Sidorkiewicz, P. Gounon, J. Dubuisson, G. Faure, R. Crainic, and A. Budkowska.** 2001. Nonenveloped nucleocapsids of hepatitis C virus in the serum of infected patients. J. Virol. **75**:8240–8250.
29. **Martire, G., A. Viola, L. Iodice, L. V. Lotti, R. Gradini, and S. Bonatti.** 2001. Hepatitis C virus structural proteins reside in the endoplasmic reticulum as well as in the intermediate compartment/*cis*-Golgi complex region of stably transfected cells. Virology **280**:176–182.
30. **Matto, M., C. M. Rice, B. Aroeti, and J. S. Glenn.** 2004. Hepatitis C virus core protein associates with detergent-resistant membranes distinct from classical plasma membrane rafts. J. Virol. **78**:12047–12053.
31. **McLauchlan, J.** 2000. Properties of the hepatitis C virus core protein: a structural protein that modulates cellular processes. J. Viral Hepat. **7**:2–14.
32. **McLauchlan, J., M. K. Lemberg, R. G. Hope, and B. Martoglio.** 2002. Intramembrane proteolysis promotes trafficking of hepatitis C virus core protein to lipid droplets. EMBO J. **21**:3980–3988.
33. **Moradpour, D., R. Gosert, D. Egger, F. Penin, H. E. Blum, and K. Bienz.** 2003. Membrane association of hepatitis C virus nonstructural proteins and identification of the membrane alteration that harbors the viral replication complex. Antivir. Res. **60**:103–109.
34. **Murphy, D. J., and J. Vance.** 1999. Mechanisms of lipid-body formation. Trends Biochem. Sci. **24**:109–115.
35. **Nakabayashi, H., K. Taketa, K. Miyano, T. Yamane, and J. Sato.** 1982. Growth of human hepatoma cells lines with differentiated functions in chemically defined medium. Cancer Res. **42**:3858–3863.
36. **Op De Beeck, A., C. Voisset, B. Bartosch, Y. Ciczora, L. Cocquerel, Z. Keck, S. Foung, F. L. Cosset, and J. Dubuisson.** 2004. Characterization of functional hepatitis C virus envelope glycoproteins. J. Virol. **78**:2994–3002.
37. **Pietschmann, T., V. Lohmann, A. Kaul, N. Krieger, G. Rinck, G. Rutter, D. Strand, and R. Bartenschlager.** 2002. Persistent and transient replication of full-length hepatitis C virus genomes in cell culture. J. Virol. **76**:4008–4021.
38. **Schweizer, A., J. A. M. Fransen, T. Bächi, L. Ginsel, and H.-P. Hauri.** 1988. Identification, by a monoclonal antibody, of a 53-kD protein associated with tubulo-vesicular compartment at the cis-side of the Golgi apparatus. J. Cell Biol. **107**:1643–1653.
39. **Schwer, B., S. Ren, T. Pietschmann, J. Kartenbeck, K. Kaehlcke, R. Bartenschlager, T. S. Yen, and M. Ott.** 2004. Targeting of hepatitis C virus core protein to mitochondria through a novel C-terminal localization motif. J. Virol. **78**:7958–7968.
40. **van Meer, G.** 2001. Caveolin, cholesterol, and lipid droplets? J. Cell Biol. **152**:29–34.
41. **Villanueva, R., Y. Rouillé, and J. Dubuisson.** 2005. Interactions between virus proteins and host cell membranes. Int. Rev. Cytol. **245**:171–244.
42. **Wakita, T., T. Pietschmann, T. Kato, T. Date, M. Miyamoto, Z. Zhao, K. Murthy, A. Habermann, H. G. Krausslich, M. Mizokami, R. Bartenschlager, and T. J. Liang.** 2005. Production of infectious hepatitis C virus in tissue culture from a cloned viral genome. Nat. Med. **11**:791–796.
43. **Yasui, K., T. Wakita, K. Tsukiyama-Kohara, S. I. Funahashi, M. Ichikawa, T. Kajita, D. Moradpour, J. R. Wands, and M. Kohara.** 1998. The native form and maturation process of hepatitis C virus core protein. J. Virol. **72**:6048–6055.
44. **Zhong, J., P. Gastaminza, G. Cheng, S. Kapadia, T. Kato, D. R. Burton, S. F. Wieland, S. L. Uprichard, T. Wakita, and F. V. Chisari.** 2005. Robust hepatitis C virus infection in vitro. Proc. Natl. Acad. Sci. USA **102**:9294–9299.

# Production of infectious genotype 1a hepatitis C virus (Hutchinson strain) in cultured human hepatoma cells

MinKyung Yi*, Rodrigo A. Villanueva*, David L. Thomas†, Takaji Wakita‡, and Stanley M. Lemon*§

*Center for Hepatitis Research, Institute for Human Infections and Immunity, and Department of Microbiology and Immunology, University of Texas Medical Branch, Galveston, TX 77555-1019; †Department of Medicine, The Johns Hopkins University, Baltimore, MD 21231; and ‡Department of Microbiology, Tokyo Metropolitan Institute for Neuroscience, Tokyo 183-8526, Japan

Communicated by Harvey J. Alter, National Institutes of Health, Bethesda, MD, December 12, 2005 (received for review November 2, 2005)

**Infections with hepatitis C virus (HCV) are marked by frequent viral persistence, chronic liver disease, and extraordinary viral genetic diversity. Although much has been learned about HCV since its discovery, progress has been slowed by a lack of permissive cell culture systems supporting its replication. Productive infections have been achieved recently with genotype 2a virus, but cirrhosis and liver cancer are typically associated with genotype 1 HCV, which is more prevalent and relatively resistant to IFN therapy. We describe production of infectious genotype 1a HCV in cells transfected with synthetic RNA derived from a prototype virus (H77-S). Viral proteins accumulated more slowly in H77-S transfected cells than in cells transfected with genotype 2a (JFH-1) RNA, but substantially more H77-S RNA was secreted into supernatant fluids. Most secreted RNA was noninfectious, banding in isopycnic gradients at a density of 1.04–1.07 gm/cm$^3$, but infectivity was associated with H77-S particles possessing a density of 1.13–1.14 gm/cm$^3$. The specific infectivity of H77-S particles ($5.4 \times 10^4$ RNA copies per focus-forming unit) was significantly lower than JFH-1 virus ($1.4 \times 10^2$ RNA copies per focus-forming unit). Infection with either virus was blocked by CD81 antibody. Sera from genotype 1a-infected individuals neutralized H77-S virus, but had little activity against genotype 2a virus, suggesting that these genotypes represent different serotypes. The ability of this genotype 1a virus to infect cultured cells will substantially benefit antiviral and vaccine discovery programs.**

bouyant density | CD81 | cell culture | neutralizing antibody | serotype

Despite intensive research efforts, many gaps remain in our understanding of hepatitis C virus (HCV) and the mechanisms by which it causes chronic liver injury (1). To a large extent, this situation reflects the absence of tractable cell culture systems that are permissive for virus replication. Recent reports describing the efficient propagation of a genotype 2a strain of HCV, JFH-1, and a related, wholly genotype 2a chimera, FL-J6/JFH, have thus stimulated much interest (2–4). The JFH-1 virus appears to be unique among strains of HCV in terms of its ability to undergo productive infection. Many aspects of the virus–host interaction, including viral entry, assembly, and release, that were previously inaccessible to experimental manipulation, can now be studied using the JFH-1 strain and its chimeric derivatives. However, the genotype 2a JFH-1 strain is not representative of the genotype 1 strains of HCV that are principally associated with liver disease in most regions of the world (5). There is thus an important need to develop systems supporting replication of other HCV genotypes in cell culture.

Like all positive-strand RNA viruses, HCV possesses an error-prone RNA replicase. Strains of HCV show extraordinary genetic diversity, both in terms of quasi-species variation within infected individuals, as well as genetic distances between viruses belonging to different genotypes (5, 6). Pairwise differences in the nucleotide sequences of the six HCV genotypes are on the order of 31–33%. This degree of variation approximates the genetic distance between members of the classical flavivirus serogroups, such as the four dengue viruses and members of the Japanese encephalitis serogroup, that represent serologically and genetically distinct viruses (7). The extent to which critical epitopes involved in antibody (Ab)-mediated neutralization varies among different HCV genotypes is not well understood. Neutralization studies using pseudotyped retrovirus particles suggest considerable relatedness among different HCV genotypes (8), but these conclusions need to be confirmed in neutralization studies using authentic HCV. There also may be important distinctions in the capacity of different genotypes of HCV to establish long-term persistence or to cause liver disease. Cirrhosis and liver cancer are typically associated with genotype 1 viruses, which are most prevalent (5). As important, there are marked differences in the therapeutic responses of different genotypes, with genotype 1 viruses being least likely (≈45%) and genotype 2 viruses most likely (≈85%) to respond to IFN-based therapy (9). Collectively, this marked genetic heterogeneity and the corresponding clinical outcome differences underscore the importance of developing genotype 1 replication systems.

Unmodified genomic RNA derived from the genotype 2a JFH-1 strain of HCV produces infectious virus particles after transfection into Huh7 hepatoma cells (2, 3). In contrast, the genome of the prototype genotype 1a virus, H77, although capable of efficient replication in chimpanzees, replicates poorly in cell culture (10, 11). Nonetheless, we recently reported the efficient replication of H77 genomic RNA containing five adaptive mutations (referred to herein as "H77-S") in Huh7 hepatoma cells (12). These adaptive mutations are located within the NS3, NS4A, and NS5A proteins (see Fig. 1*A*). Here, we describe production of infectious HCV in cells transfected with this RNA. We compare the biophysical properties of genotype 1a and 2a particles produced in cell culture and show that these viruses can be readily distinguished serologically. Although possessing lower specific infectivity than JFH-1 virus produced in cell culture, the ability of this genotype 1a virus to infect cultured cells should substantially benefit antiviral and vaccine discovery programs.

## Results

Previous studies have shown that a combination of five cell culture-adaptive mutations provide for efficient replication of the genotype 1a H77-S RNA in transfected Huh7 cells (12). To assess the ability of this highly cell-culture-adapted RNA to produce infectious virus in transfected cells, we created a related mutant, H77-S/ΔE1p7, with an in-frame deletion of sequence encoding the HCV structural proteins, E1, E2, and p7, that should eliminate virus particle formation but not impair viral RNA replication (Fig. 1*A*). Synthetic RNA transcribed from these two constructs, and an RNA replication-defective mutant containing an Ala–Ala–Gly substitution for the conserved Gly–

Conflict of interest statement: No conflicts declared.

Abbreviations: FFU, focus-forming unit; HCV, hepatitis C virus.

§To whom correspondence should be addressed at: Center for Hepatitis Research, Institute for Human Infections and Immunity, University of Texas Medical Branch, 301 University Boulevard, Galveston, TX 77555-1019. E-mail: smlemon@utmb.edu.





www.pnas.org/cgi/doi/10.1073/pnas.0510727103

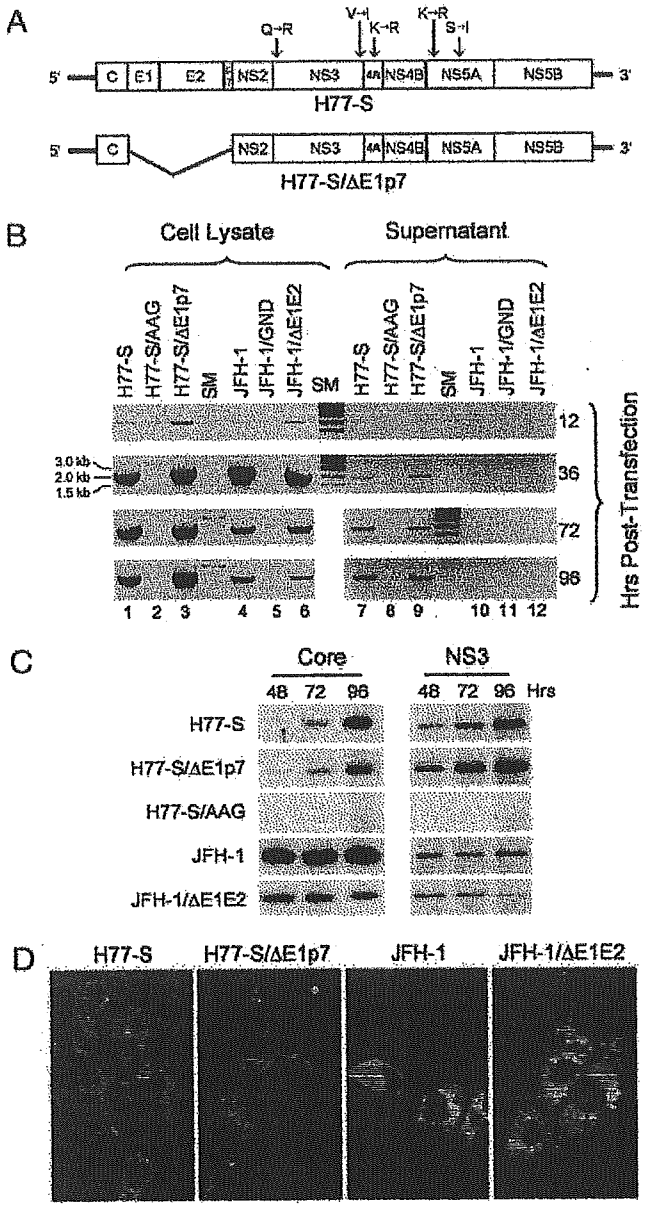


**Fig. 1.** Replication of H77-S and JFH-1 RNAs in transfected Huh-7.5 cells. (*A*) Organization of the H77-S genomic RNA, showing location of the five adaptive mutations and the H77-S/ΔE1p7 mutant in which sequence encoding the structural proteins was deleted. (*B*) Semiquantitative RT-PCR assays for HCV RNA in lysates (*Left*) and supernatant fluids (*Right*) of transfected Huh-7.5 cells. (*C*) Immunoblot detection of the HCV core and NS3 proteins in transfected Huh-7.5 cells. (*D*) Core antigen detected by indirect immunofluorescence 96 h after transfection of Huh-7.5 cells with the indicated RNA.

Asp–Asp motif in the NS5B polymerase active site (H77-S/AAG), were electroporated into Huh-7.5 cells. These cells are deficient in signaling virus activation of IFN-β synthesis through the intracellular retinoic acid-inducible gene I (RIG-I) pathway and are highly permissive for HCV RNA replication (13, 14). In parallel, Huh-7.5 cells were transfected with similar RNA transcripts derived from the JFH-1 virus and related mutants containing either a deletion of E1 and E2 or a Gly–Asn–Asp substitution in NS5B. Cells were monitored for replication of the transfected RNAs by a semiquantitative RT-PCR assay targeting an ≈1.9-kb segment of the NS3-coding region (see *Materials and Methods*). This assay is sensitive and specific for replication of synthetic viral RNAs after transfection.

Both the H77-S and JFH-1 RNAs replicated efficiently in Huh-7.5 cells, as did the related mutants in which the structural proteins were deleted (Fig. 1*B*, lanes 1, 3 and 4, 6). RNA synthesis was evident as early as 12 h after electroporation, with strong RT-PCR signals obtained from lysates prepared 36 h after transfection. These levels of RNA persisted in the H77-S and H77/S-ΔE1p7 transfected cells through 96 h after transfection (lanes 1 and 3), whereas the RT-PCR signal was notably decreased in JFH-1 and JFH-1/ΔE1E2-transfected cells by 72–96 h compared with that present at 36 h (lanes 4 and 6). In contrast, viral RNA was not detected in lysates of cells transfected with the NS5B mutants, indicating a failure of replication (Fig. 1*B*, lanes 2 and 5). These results were confirmed by immunoblot detection of the core and NS3 proteins in lysates of the transfected cells (Fig. 1*C*) and by immunofluorescence imaging of the core protein (Fig. 1*D*).

Several interesting differences were apparent in the expression of H77-S and JFH-1 proteins. Despite high abundance of viral RNA in H77-S transfected cells (Fig. 1*B*), JFH-1 transfected cells contained substantially more core protein, particularly at early time points (Fig. 1*C*). Core accumulated slowly in H77-S transfected cells, whereas its abundance was maximal at the earliest time point, 48 h, in JFH-1 transfected cells. Immunofluorescence staining was also substantially more intense for core antigen in the JFH-1 transfected cells (Fig. 1*D*). NS3 abundance also increased with time in H77-S transfected cells, whereas maximal levels were present at 48 h in JFH-1 transfected cells (Fig. 1*C*). The less intense NS3 signal in JFH-1 immunoblots likely reflects antigenic differences between JFH-1 and H77-S, as the NS3 Ab was raised to genotype 1a protein. In contrast, the anti-core monoclonal Ab (mAb) we used recognizes an epitope located between residues 21–40 of the protein, which is conserved in both viruses. These results suggest that JFH-1 RNA produces more core protein than H77-S RNA or that the JFH-1 core protein has greater stability than the H77-S protein in Huh-7.5 cells. However, a smaller proportion of cells expressed detectable core antigen in the JFH-1 transfected cultures 96 h after transfection (Fig. 1*D*). This difference suggests that JFH-1 RNA replication may be associated with greater cell death than H77-S.

Because Huh7 cells transfected with the JFH-1 RNA are known to release infectious virus particles (2, 3), we compared the secretion of viral RNA from these cells into the supernatant culture fluids. Substantially more viral RNA was released into supernatant fluids from H77-S transfected cells than from JFH-1 transfected cells (Fig. 1*B*, compare lanes 7 and 10), with the abundance of H77-S RNA released increasing between 36 and 96 h. In contrast, JFH-1 RNA release was minimal and detected only at 36 h after transfection in this assay. However, the release of either of these RNAs into the supernatant fluids was not dependent on expression of the envelope proteins (lanes 9 and 12), indicating that the presence of viral RNA in the culture media is not indicative of viral particle assembly.

Clarified supernatant culture fluids collected 24–96 h after transfection were tested for the presence of infectious virus by inoculation onto naïve Huh-7.5 cells, followed by fixation and staining for the presence of core antigen 96 h later. Core was present in numerous cells inoculated with the JFH-1 supernatant fluids (Fig. 2*A Right*), consistent with infection with JFH-1 virus (2, 3). Importantly, we also observed core antigen in a smaller number of cells inoculated with the H77-S supernatant fluids (Fig. 2. *Left*). As described previously for the JFH-1 virus (2), H77-S infected cells were grouped in small clusters. These clusters appear to result from division of a single infected cell during the 96-h incubation period or possibly by cell-to-cell spread of virus. Thus, in subsequent experiments, we measured virus infectivity in terms of "focus-forming units" (FFU). Im-

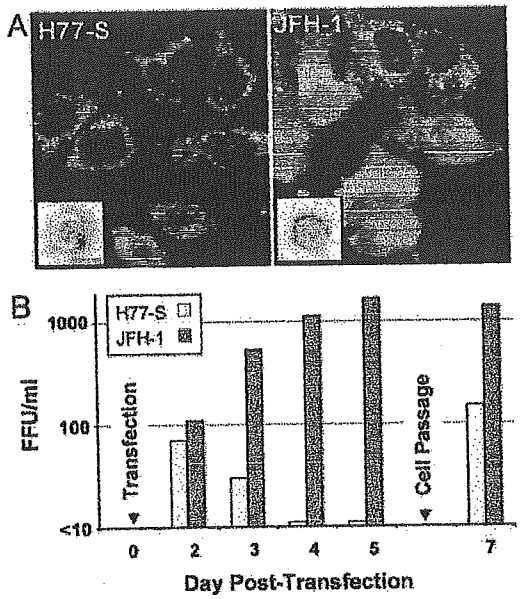


Fig. 2. Infection of Huh-7.5 cells with H77-S and JFH-1 virus released into supernatant fluids of transfected Huh-7.5 cells. (*A*) HCV core antigen expression in cells infected with H77-S (*Left*) or JFH-1 (*Right*) virus. *Left Inset* shows a particle with immunogold labeling indicating recognition by the AP33 mAb to E2. (Bar: 50 nm.) *Right Inset* shows a typical JFH-1 particle for comparison. (See also Fig. 5.) (*B*) Time course of infectious H77-S (open bars) and JFH-1 (filled bars) virus released into supernatant fluids of RNA-transfected Huh-7.5 cells. H77-S release was greatest 24–48 h after transfection or passage of cells.

portantly, the intensity of antigen staining in these cells mirrored that in the transfected Huh-7.5 cells, with less intense staining of core antigen in H77-S infected cells. Supernatant fluids remained infectious after passage through a 0.2-$\mu$m filter, consistent with cell-free virus.

Interestingly, the release of infectious virus from H77-S transfected cells was not continuous, but was greatest 24–48 h after transfection and reduced subsequently (Fig. 2*B*). Trypsin treatment of the cell monolayer, followed by a 1:3 split and reseeding of the cells at a lower density, resulted in a reproducible burst of virus production. These results are consistent with previous observations indicating that HCV RNA replication is tightly coupled to host cell proliferation and that viral RNA synthesis is enhanced during the S phase of the cell cycle (15, 16). In contrast, the release of JFH-1 virus was continuous and increased with time (Fig. 2*B*).

Electron microscopic examination of supernatant fluids from both H77-S- and JFH-1-transfected cultures revealed the presence of occasional virus-like particles measuring 44–64 nm in diameter (Fig. 2*A Insets*; see also Fig. 5, which is published as supporting information on the PNAS web site). Some particles in the H77-S infectious material bound gold-labeled mAbs to the E2 glycoprotein of HCV (Fig. 2*A Left Inset*). Importantly, neither viral antigen expression in inoculated cells nor virus-like particles were observed with supernatant fluids taken from cells transfected with the H77-S/ΔE1p7 mutant, despite equivalently robust replication of that RNA in transfected cells (Fig. 1*B*, lanes 3 and 9). Together, these results provide strong evidence for the production of cell culture-infectious H77-S virus in transfected Huh-7.5 cells. However, the lower number of antigen-positive cells obtained with inoculation of the H77-S harvest compared with the JFH-1 harvest suggests that the production of infectious virus is 10- to 100-fold less efficient with H77-S.

To compare the physical properties of infectious H77-S and JFH-1 particles, aliquots of concentrated posttransfection supernatant fluids were passed through a 0.2-$\mu$m filter and then layered onto a preformed 10–40% iodixanol gradient, which was centrifuged to equilibrium. Fractions collected from this isopycnic gradient were tested for viral RNA by the semiquantitative RT-PCR assay described above (Fig. 3*A*). Much of the H77-S RNA was present in fractions 2 to 3, near the top of the gradient, but a major fraction of the RNA banded discreetly at a higher density (≈1.13–1.14 g/cm$^3$) in fractions 5 to 6. Importantly, this second RNA peak was absent in gradients loaded with concentrated supernatant fluids from cells transfected with the H77-S/ΔE1p7 mutant (Fig. 3*A*). Although a small amount of JFH-1

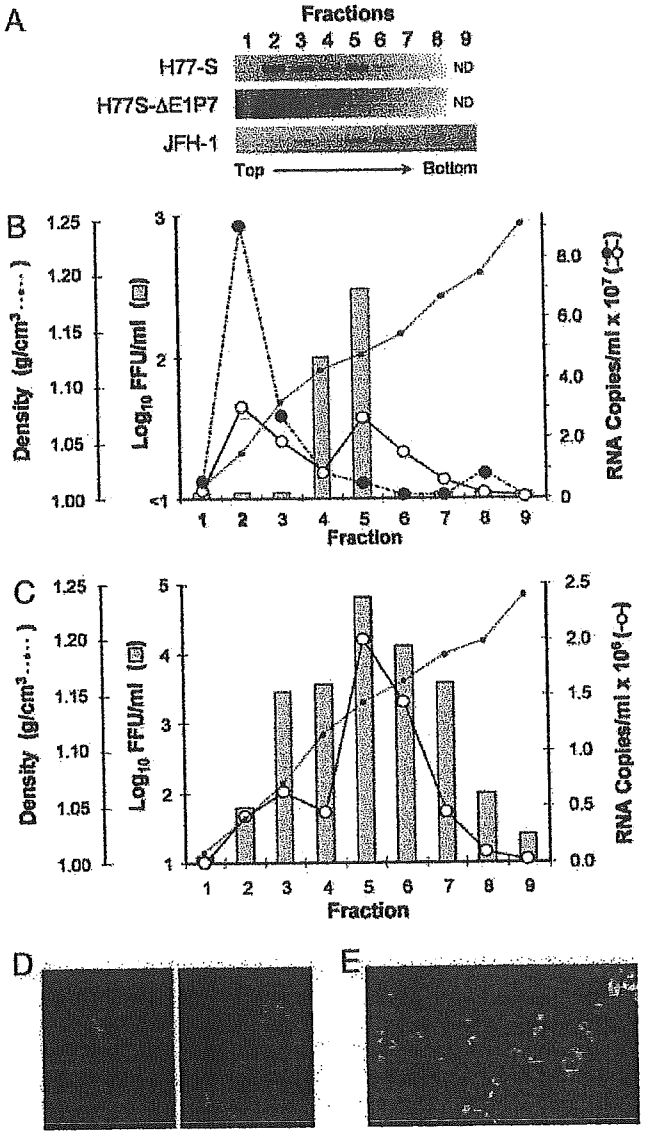


Fig. 3. Equilibrium ultracentrifugation of H77-S and JFH-1 particles in isopycnic iodixanol gradients. (*A*) Semiquantitative RT-PCR detection of HCV RNA in fractions of gradients loaded with concentrated, filtered (0.2 $\mu$m) supernatant fluids from cells transfected with the indicated RNAs. (*B*) Results of infectivity assays (bars) and quantitative TaqMan RT-PCR assays in fractions from gradients loaded with concentrated supernatant fluids from cells transfected with H77-S (solid line with open circles) or H77-S/ΔE1p7 (dashed line with filled circles) RNA. H77-S/ΔE1p7 supernatant fluids contained no infectious virus. (*C*) Results of similar assays using fractions from gradients loaded with concentrated JFH-1 supernatant fluids. (*D* and *E*) HCV core antigen detected by indirect immunofluorescence in cells inoculated with fraction 5 of gradients loaded with H77-S (*D*) or JFH-1 (*E*) material (lower magnification).

RNA was detectable in fraction 3, most was present in fractions 5 to 6 (Fig. 3*A*). These results were confirmed by real-time quantitative RT-PCR assays targeting a small, conserved segment of the 5′ nontranslated RNA (Fig. 3 *B* and *C*). When fractions were inoculated onto naïve Huh-7.5 cells, H77-S infectivity was found only in fractions 4 and 5, whereas the maximum JFH-1 infectivity was present in fraction 5 (Fig. 3*B*). No infectious virus was present in supernatant fluids from the H77-S/ΔE1p7 transfected cells. The intensity of core antigen staining in cells infected with the H77-S and JFH-1 virus from these gradients showed the characteristic difference in staining intensity described above (Fig. *3*, compare *D* and *E*). These results indicate that infectious H77-S virus has a buoyant density similar to that of JFH-1 virus: ≈1.13–1.14 g/cm$^3$.

We estimated the specific infectivity of the JFH-1 and H77-S viruses banding at this density by comparing the abundance of viral RNA in these fractions (determined by real-time RT-PCR) with the infectious titer. These results suggested a specific infectivity of 140 ± 13 S.E. RNA copies per FFU for the JFH-1 virus, compared with 54,000 ± 18,000 copies per FFU for the H77 virus (based on analysis of three fractions in two independent experiments). Thus, the JFH-1 virus has ≈400-fold greater specific infectivity than the H77-S virus in these fractions. The magnitude of this difference cannot be explained by differences in the ability of the RT-PCR assay to detect JFH-1 vs. H77-S RNA, nor is it likely to be due to contamination of the H77-S virus in fractions 4 and 5 with the RNA peaking in fraction 2 of the gradient that was not associated with infectious virus (Fig. 3*B*).

Because synthetic RNA transcripts banded at a higher density than infectious virus in these gradients (1.15–1.17 g/cm$^3$; data not shown), it is likely that the noninfectious H77-S RNA in fractions 2–3 is present in membranous complexes. The possibility that this material might be derived from viral replicase complexes is suggested by the presence of NS3 and NS5B within these fractions (see Fig. 6, which is published as supporting information on the PNAS web site). The abundance of E2 and core protein was not sufficient in fractions containing infectious virus for reproducible detection by immunoblot.

To characterize further the infectious particles produced in H77-S transfected cells, we carried out neutralization assays using serum samples collected prospectively from injection drug users who had experienced acute genotype 1 HCV infection (17). Dilutions of each serum sample were mixed with a fixed amount of H77-S, incubated for 60 min, then inoculated onto naïve Huh-7.5 cells. A >50% reduction in FFU was considered indicative of virus neutralizing Abs. We tested paired sera from three subjects, collected before and 8–14 months after initial serologic evidence of HCV infection. As shown in Fig. 4*A Upper*), none of the preinfection sera neutralized >50% of the H77-S inoculum, at any dilution, whereas a 1:10 dilution of each of the postinfection sera resulted in an 87–97% reduction in FFU relative to either the paired preinfection specimen, or a no serum control (98 ± 7 FFU). Fifty percent neutralization endpoints for the postinfection sera ranged from 1:700 to >1:1250. The specific neutralization of H77-S infectivity with postinfection human sera confirms that the infectious particles produced by H77-S transfected cells are antigenically related to those produced during human infections with wild-type virus. We also tested these sera for the ability to neutralize JFH-1 virus (Fig. 4*A Lower*). Only one of the three postinfection sera (patient no. 455) was capable of neutralizing JFH-1 virus (titer = 1:40), indicating substantial serologic differences between these two viruses.

CD81 is expressed on the surface of many cells and has been shown to interact with the E2 protein of HCV (18). Abs to CD81 block the infection of Huh7 cells with HCV pseudotyped retroviral particles, as well as the genotype 2a JFH-1 virus (2, 3, 19). Moreover, a soluble CD81 fragment blocks infection of hepatoma cells with the FL-J6/JFH chimera (4). We found that

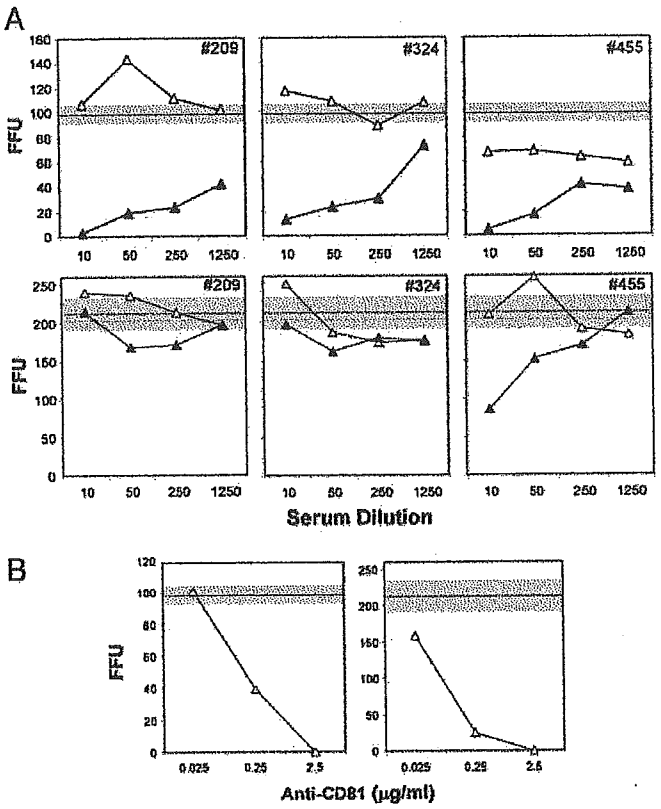


**Fig. 4.** Neutralization of cell culture-produced virus infectivity by antibody to HCV or CD81. (*A*) Neutralization of H77-S (*Upper*) and JFH-1 (*Lower*) viruses by paired preinfection (△) or after seroconversion (▲) sera from three individuals sustaining infection with genotype 1a HCV. The horizontal lines and shaded zones indicate the mean and range of infectious foci obtained with each viral inoculum in the absence of any serum. (*B*) Anti-CD81 Ab, added to virus before its inoculation onto Huh-7.5 cells, prevents infection with either H77-S (*Left*) or JFH-1 (*Right*) inocula.

anti-CD81 Ab efficiently blocked the infection of Huh-7.5 cells with H77-S virus (Fig. 4*B Left*). These data suggest that H77-S and JFH-1 particles bind to and enter Huh-7.5 cells by similar mechanisms, most likely involving virus recognition of the CD81 molecule on the cell surface.

## Discussion

Until recently, efforts to study HCV and its interactions with host cells have been impeded by the absence of cell culture systems that are capable of supporting all stages of the virus life cycle. The development of efficiently replicating subgenomic RNA replicons and genome-length selectable RNAs has been helpful in providing model systems that recapitulate events in viral polyprotein expression, processing, replicase assembly, and viral RNA synthesis (20–22). However, these experimental systems are not capable of providing insights into interactions of the virus with host-cell receptors, the process of viral entry, or assembly and release from the cell. The recent recognition that the genotype 2a virus, JFH-1, is capable of very efficient RNA replication as well as the production of fully infectious virus particles in transfected cells thus represents a major breakthrough for the hepatitis C field.

Our demonstration here of the ability of the H77-S virus to undergo the complete viral life cycle in Huh7.5 cells represents another important step in the development of useful cell culture systems for HCV. Unlike the genotype 2a JFH-1 virus, the genotype 1a H77-S virus is representative of the most prevalent

HCV genotypes causing liver disease within the United States, as well as many other countries (5, 6). It carries five defined cell culture-adaptive mutations that distinguish it from the prototype Hutchinson strain (H77C) virus that is highly infectious for chimpanzees and that has been used in many early studies characterizing HCV (10, 12, 23). The adaptive mutations in H77-S that promote efficient viral RNA replication are located within the NS3/4A protease complex and the NS5A protein, a nonstructural phosphoprotein (12). Both of these proteins appear to be essential components of the viral RNA replicase, but both proteins also play important roles in confounding innate cellular antiviral defenses (24, 25). How these five adaptive mutations modulate these viral functions to promote HCV RNA replication remains unknown, as is their impact, if any, on viral assembly and release. It will be interesting to determine whether these mutations reduce the ability of the virus to infect chimpanzees; previous studies with a genotype 1b virus suggest mutations that promote RNA replication in cultured cells reduce the ability of the virus to infect chimpanzees (26).

Although the lower quantities of infectious H77-S virus released from transfected cells correlates well with the lower abundance of viral proteins expressed, compared with JFH-1 transfected cells (Fig. 1*C*), the production of infectious virus does not appear to be determined only by the cellular abundance of HCV RNA and/or its proteins. In other studies, we could not detect release of infectious virus from cells transfected with a highly cell culture-adapted, genotype 1b RNA derived from HCV-N (22), despite the expression of viral RNA and proteins roughly comparable with that observed with H77-S (M.Y. and S.M.L., unpublished data).

Quantitatively more viral RNA was released from H77-S transfected cells than JFH-1 transfected cells, but most of this RNA banded at a very low density in iodixanol gradients (≈1.03–1.07 g/ml) (Fig. 3*B*). This RNA was not naked viral RNA, which possesses a significantly higher density (1.15–1.17 g/ml) (data not shown). The nature of the low-density RNA is uncertain. It may represent only membrane-bound RNA associated with replication complexes released from dying cells, as suggested by the presence of NS3 and NS5B in these fractions (Fig. 6). It is interesting to note, however, that some circulating HCV RNA molecules present in human sera are found at a density of ≈1.06 gm/cm$^3$ after equilibrium ultracentrifugation (27), suggesting that the low-density RNA released from H77-S transfected cells may have possible physiologic relevance.

The much lower specific infectivity of the H77-S particles banding at 1.13–1.14 gm/cm$^3$, compared with JFH-1 particles with the same density, also remains to be explained. Both viral RNAs appear to replicate efficiently in transfected cells (Fig. 1*B*), but the structural and nonstructural proteins accumulate more slowly in H77-S transfected cells (Fig. 1*C*). To document the presence of core antigen in H77-S infected cells, we were required to incubate cells for 96 h after inoculation with virus. In contrast, abundant core antigen was present in JFH-1 infected cells by 48 h. It is tempting to speculate that this difference might explain, at least in part, the 400-fold difference we observed in the specific infectivity of JFH-1 and H77-S particles. However, a specific defect in virus entry or uncoating cannot be excluded. Widely different cell entry efficiencies have been observed with pseudotyped retroviruses bearing envelope glycoproteins from different HCV strains (19).

Although further work will be required to answer these and many other questions, the availability of a genotype 1a virus that is capable of undergoing the complete viral cycle in cultured cells should be a major asset to the hepatitis C field. The widely divergent neutralizing Ab activities we found against genotype 1a and 2a viruses in human sera (Fig. 4*A*) suggest that these viruses may represent distinct serotypes, an observation that has significant implications for vaccine development.

## Materials and Methods

**Plasmids.** The H77-S virus was derived from the chimpanzee-infectious genotype 1a pCV-H77C cDNA clone (GenBank accession no. AF011751) (10). It contains five cell culture-adaptive mutations, two within NS3 (Q1067R, V1651I), one in NS4A (K1691R), and two in NS5A (K2040R, S2204I) (12). Construction of pH77-S, formerly called pH77c/QR/VI/KR/KR$^{5A}$/SI, as well as the related replication-defective NS5B mutant, H77-S/AAG, has been described (12). pH77-S/ΔE1p7 contains an in-frame deletion spanning the E1-p7 coding (see *Supporting Materials and Methods*, which is published as supporting information on the PNAS web site). The JFH-1, JFH-1/GND, and JFH-1/ΔE1E2 plasmids are described in ref. 3.

**Cells.** The Huh7 cell subline, Huh-7.5, was kindly provided by Charles Rice (Rockefeller University, New York) (13). Cells were cultured as described in ref. 12.

**Abs.** H53 mAb to E2 was a gift from J. Dubuisson (Institut de Biologie de Lille/Institut Pasteur de Lille, Lille, France) (28); the AP33 mAb was kindly provided by A. Patel (Medical Research Council Virology Unit, University of Glasgow, Glasgow, U.K.) (29). Human sera were provided by D. Netski (The Johns Hopkins University, Baltimore) (17). Commercial Abs included anti-core C7–50 (Affinity BioReagents, Golden, CO), anti-NS3 BDI371 (BioDesign, Saco, ME), and anti-CD81 JS-81 (BD Pharmingen).

**HCV RNA Transfection and Virus Production.** HCV RNAs were transcribed *in vitro* and electroporated into cells as described in ref. 12. In brief, 10 μg of *in vitro* synthesized HCV RNA was mixed with 5 × 10$^6$ Huh-7.5 cells in a 2-mm cuvette and pulsed twice at 1.4 kV and 25 μF. Cells were seeded into 12-well plates for RNA analysis or 6-well plates for protein analysis. For virus production, transfected cells were seeded into 75 cm$^2$ flasks and fed with medium containing 10% FCS. These cells were passaged with a 3:1 split at 3–4 days after transfection. Twenty-four hours later, the medium was replaced with serum-free medium, which was collected 24 h later as the virus harvest. Virus harvests were clarified by low-speed centrifugation and, where indicated, passed through a 0.2-μm filter before stabilization by addition of 20% FCS and freezing at −80°C.

**Infectivity Assays.** Huh-7.5 cells were seeded at 2 × 10$^4$ cells/well in 8-well chamber slides (Nalge Nunc, Rochester, NY) 24 h before inoculation with 80–100 μl of culture medium or gradient fractions (see below). Cells were tested for the presence of intracellular core antigen by immunofluorescence 96 h later (48 h for JFH-1 virus), as described below. Clusters of infected cells identified by staining for core antigen were considered to constitute a single infectious focus, and virus titers were calculated accordingly in terms of FFU/ml.

**Immunofluorescence Detection of Intracellular HCV Antigen.** Cells were fixed in methanol:acetone (1:1) at room temperature for 9 min, then stained with mAb C7–50 to the core protein diluted 1:300, followed by extensive washing and staining with FITC-conjugated goat anti-mouse IgG Ab (1010-02, Southern Biotech, Birmingham, AL) at a 1:100 dilution. Nuclei were counterstained with Bisbenzimide H (Hoechst, Frankfurt am Main, Germany), and slides were examined with a Zeiss LSM 510 laser scanning confocal microscope.

**Neutralization Assay.** Virus stock containing ≈2 × 10$^3$ FFU/ml virus was mixed with an equal volume of serial dilutions of heat-inactivated (56°C for 30 min) human sera and incubated at 37°C for 1 h before inoculation onto Huh-7.5 cells in 8-well chamber slides, as described above. After incubation of the

cultures for 48 (JFH-1) or 96 (H77-S) h, cells were fixed and stained for the presence of HCV core antigen by indirect immunofluorescence (see above), and the foci of antigen-positive cells were enumerated. A >50% reduction in FFU (compared with virus incubated with no serum) was considered indicative of neutralizing Ab; endpoint 50% neutralization titers were estimated by using the least-squares method.

**Equilibrium Ultracentrifugation.** Filtered supernatant fluids collected from transfected cell cultures (no FCS) were concentrated 20- to 50-fold by using a Centricon PBHK Centrifugal Plus-20 Filter Unit with Ultracel PL membrane (100-kDa exclusion) (Millipore), then layered on top of a preformed continuous 10–40% iodixanol (OptiPrep, Sigma-Aldrich) gradient in Hanks' balanced salt solution (HBSS; Invitrogen). Gradients were centrifuged in a SW60 rotor (Beckman Coulter) at 45,000 rpm for 16 h at 4°C, and fractions (500 $\mu$l each) were collected from the top of the tube. The density of each fraction was estimated by weighing a 100-$\mu$l drop from fractions of a gradient run in parallel but loaded with HBSS.

**Quantitation of HCV RNA.** Both semiquantitative and quantitative real-time RT-PCR assays were used to determine the abundance of viral RNA in transfected cells and virus harvests. For details, see *Supporting Materials and Methods*.

**Immunoblot Analysis.** Blots were incubated with Abs to core (C7–50, 1:30,000) or NS3 (BDI371, 1:20,000), followed by horseradish peroxidase-conjugated anti-mouse IgG (1030-05, Southern Biotech) (1:30,000). Proteins were visualized by chemiluminesence using reagents provided with the ECL Advance kit (Amersham Pharmacia Biosciences).

We thank Robert Purcell and Jens Bukh (both of the National Institutes of Health, Bethesda) for the pCV-H77C plasmid; Charles Rice for Huh7.5 cells; and Dale Netski, Jean Dubuisson, and Arvind Patel for human sera and mAbs. We thank Vsevolod Popov for technical advice, Jeremy Yates and Francis Bodola for excellent technical assistance, and Annette Martin for critically reviewing the manuscript. This work was supported by National Institute of Allergy and Infectious Diseases Grants U19-AI40035, R21-AI063451, and N01-AI25488.

1. Chisari, F. V. (2005) *Nature* **436,** 930–932.
2. Zhong, J., Gastaminza, P., Cheng, G., Kapadia, S., Kato, T., Burton, D. R., Wieland, S. F., Uprichard, S. L., Wakita, T. & Chisari, F. V. (2005) *Proc. Natl. Acad. Sci. USA* **102,** 9294–9299.
3. Wakita, T., Pietschmann, T., Kato, T., Date, T., Miyamoto, M., Zhao, Z., Murthy, K., Habermann, A., Krauslich, H.-G., Mizokami, M., *et al.* (2005) *Nat. Med.* **11,** 791–796.
4. Lindenbach, B. D., Evans, M. J., Syder, A. J., Wolk, B., Tellinghuisen, T. L., Liu, C. C., Maruyama, T., Hynes, R. O., Burton, D. R., McKeating, J. A., *et al.* (2005) *Science* **309,** 623–626.
5. Zein, N. N. (2000) *Clin. Microbiol. Rev.* **13,** 223–235.
6. Simmonds, P., Bukh, J., Combet, C., Deleage, G., Enomoto, N., Feinstone, S., Halfon, P., Inchauspe, G., Kuiken, C., Maertens, G., *et al.* (2005) *Hepatology* **42,** 962–973.
7. Zanotto, P. M., Gould, E. A., Gao, G. F., Harvey, P. H. & Holmes, E. C. (1996) *Proc. Natl. Acad. Sci. USA* **93,** 548–553.
8. Logvinoff, C., Major, M. E., Oldach, D., Heyward, S., Talal, A., Balfe, P., Feinstone, S. M., Alter, H., Rice, C. M. & McKeating, J. A. (2004) *Proc. Natl. Acad. Sci. USA* **101,** 10149–10154.
9. National Institutes of Health Consensus Development Panel (2002) *NIH Consensus Statement on Management of Hepatitis C,* NIH Consensus State Science Statements (Natl. Inst. of Health, Bethesda), Vol. 19, pp. 1–46.
10. Yanagi, M., Purcell, R. H., Emerson, S. U. & Bukh, J. (1997) *Proc. Natl. Acad. Sci. USA* **97,** 8738–8743.
11. Blight, K. J., McKeating, J. A., Marcotrigiano, J. & Rice, C. M. (2003) *J. Virol.* **77,** 3181–3190.
12. Yi, M. & Lemon, S. M. (2004) *J. Virol.* **78,** 7904–7915.
13. Blight, K. J., McKeating, J. A. & Rice, C. M. (2002) *J. Virol.* **76,** 13001–13014.
14. Sumpter, R., Jr., Loo, M. Y., Foy, E., Li, K., Yoneyama, M., Fujita, T., Lemon, S. M. & Gale, M. J., Jr. (2005) *J. Virol.* **79,** 2689–2699.
15. Pietschmann, T., Lohmann, V., Rutter, G., Kurpanek, K. & Bartenschlager, R. (2001) *J. Virol.* **75,** 1252–1264.
16. Scholle, F., Li, K., Bodola, F., Ikeda, M., Luxon, B. A. & Lemon, S. M. (2004) *J. Virol.* **78,** 1513–1524.
17. Netski, D. M., Mosbruger, T., Depla, E., Maertens, G., Ray, S. C., Hamilton, R. G., Roundtree, S., Thomas, D. L., McKeating, J. & Cox, A. (2005) *Clin. Infect. Dis.* **41,** 667–675.
18. Pileri, P., Uematsu, Y., Campagnoli, S., Galli, G., Falugi, F., Petracca, R., Weiner, A. J., Houghton, M., Rosa, D., Grandi, G., *et al.* (1998) *Science* **282,** 938–941.
19. McKeating, J. A., Zhang, L. Q., Logvinoff, C., Flint, M., Zhang, J., Yu, J., Butera, D., Ho, D. D., Dustin, L. B., Rice, C. M., *et al.* (2004) *J. Virol.* **78,** 8496–8505.
20. Lohmann, V., Korner, F., Koch, J., Herian, U., Theilmann, L. & Bartenschlager, R. (1999) *Science* **285,** 110–113.
21. Blight, K. J., Kolykhalov, A. A. & Rice, C. M. (2000) *Science* **290,** 1972–1974.
22. Ikeda, M., Yi, M., Li, K. & Lemon, S. M. (2002) *J. Virol.* **76,** 2997–3006.
23. Feinstone, S. M., Alter, H. J., Dienes, H. P., Shimizu, Y., Popper, H., Blackmore, D., Sly, D., London, W. T. & Purcell, R. H. (1981) *J. Infect. Dis.* **144,** 588–598.
24. Lindenbach, B. D. & Rice, C. M. (2005) *Nature* **436,** 933–938.
25. Gale, M., Jr., & Foy, E. M. (2005) *Nature* **436,** 939–945.
26. Bukh, J., Pietschmann, T., Lohmann, V., Krieger, N., Faulk, K., Engle, R. E., Govindarajan, S., Shapiro, M., St Claire, M. & Bartenschlager, R. (2002) *Proc. Natl. Acad. Sci. USA* **99,** 14416–14421.
27. Hijikata, M., Shimizu, Y. K., Kato, H., Iwamoto, A., Shih, J. W., Alter, H. J., Purcell, R. H. & Yoshikura, H. (1993) *J. Virol.* **67,** 1953–1958.
28. Op De Beeck, A., Voisset, C., Bartosch, B., Ciczora, Y., Cocquerel, L., Keck, Z., Foung, S., Cosset, F. L. & Dubuisson, J. (2004) *J. Virol.* **78,** 2994–3002.
29. Owsianka, A., Tarr, A. W., Juttla, V. S., Lavillette, D., Bartosch, B., Cosset, F. L., Ball, J. K. & Patel, A. H. (2005) *J. Virol.* **79,** 11095–11104.

Pathophysiology

Intervirology

Intervirology 2006;49:37–43
DOI: 10.1159/000087261

# Comparison between Subgenomic Replicons of Hepatitis C Virus Genotypes 2a (JFH-1) and 1b (Con1 NK5.1)

Michiko Miyamoto[a] Takanobu Kato[a, b] Tomoko Date[a] Masashi Mizokami[b] Takaji Wakita[a]

[a]Department of Microbiology, Tokyo Metropolitan Institute for Neuroscience, Tokyo, and
[b]Department of Clinical Molecular Informative Medicine, Nagoya City University Graduate School of Medical Sciences, Nagoya, Japan

**Key Words**
Genotypes · Hepatitis C virus · Interferon · Replicon

**Abstract**
Although replicon systems for hepatitis C virus (HCV) recently developed have enabled the replication of HCV in cultured cells, limited genotypes are available for them. We have isolated HCV cDNA of genotype 2a (JFH-1 strain) from serum of a patient with fulminant hepatitis. A subgenomic replicon of JFH-1 was constructed and compared with the HCV replicon of genotype 1b (Con1 NK5.1) which possessed adaptive mutations. Huh7 cells transfected with replicon RNAs that had been transcribed in vitro were cultured in the presence of neomycin sulfate (G418), and selected colonies were isolated and expanded. Then, growth rates and replication of HCV RNA were evaluated on isolated cells hosting replicons. Saturation densities were lower for cells propagating JFH-1 than Con1 NK5.1 or untransfected Huh7 cells, and the mean doubling time was longer for JFH-1 than for Huh7 cells. Levels of HCV RNA replication in isolated clones were similar between JFH-1 and Con1 NK5.1 cells. Replication of RNA decreased reciprocally with cell densities in both JFH-1 and Con1 NK5.1 cells. The replication of HCV RNA was more resistant to interferon-α in JFH-1 than in Con1 NK5.1 cells based on the comparison of an inhibitory concentration of 50%. In conclusion, we found differences between HCV replicon clones of genotypes 1b and 2a. However, these differences may result from strain-specific characteristics, such as the source of HCV, rather than characteristics of distinct genotypes. Therefore, further investigation may be needed on more HCV isolates of diverse genotypes.



## Introduction

Hepatitis C virus (HCV) is a positive-strand RNA virus categorized in a flavivirus by structural similarities. The genomic RNA of HCV comprises approximately 9,600 nucleotides encoding a single open reading frame encoding about 3,000 amino acid residues [1–4]. HCV displays marked genetic heterogeneity and is currently classified into six major genotypes which are broken down into many subgroups [5]. Some HCV genotypes have regional distribution, and of those, genotypes 1 and 2 occur worldwide. In Japan, genotype 1b is the most frequent genotype, followed by genotype 2a [6]. Differences be-

KARGER
Fax +41 61 306 12 34
E-Mail karger@karger.ch
www.karger.com


0300–5526/06/0492–0037$23.50/0

Accessible online at:
www.karger.com/int

Takaji Wakita, MD
Department of Microbiology, Tokyo Metropolitan Institute for Neuroscience
2-6 Musashidai, Fuchu-shi
Tokyo 183-8526 (Japan)
Tel. +81 42 325 3881, ext. 4605, Fax +81 42 321 8678, E-Mail wakita@tmin.ac.jp

tween these two HCV genotypes have been noted in clinical profiles, severity of liver disease, and most importantly, response to antiviral therapies [7]. These clinical differences may be due to viral characteristics, and systems to deepen the understanding of molecular mechanisms underlying such differences have been proposed.

Lohmann et al. [8] reported subgenomic replicons of HCV RNA selectable by neomycin sulfate (G418) which can autonomously replicate in Huh7 cells. This system provides a novel powerful tool for studying mechanisms of HCV replication and selecting potential antiviral agents. Despite big advantages of this system, replication-competent replicons have been engineered only from HCV isolates of genotype 1 [8–11]. Recently, we established a subgenomic HCV replicon derived from the JFH-1 clone of genotype 2a, which had been isolated from a patient with fulminant hepatitis [12]. The JFH-1 replicon system has high efficiency in colony formation and robust RNA replication not only in Huh7 cells, but also in other liver-derived cell lines such as HepG2 and IMY-N9 [13], as well as nonhepatic cell lines like HeLa and 293 cells [14]. The availability of this replicon has enabled comparison in replication between replicons of distinct genotypes in cultured cells. The aim of the present study is to compare JFH-1 (genotype 2a) and Con1 NK5.1 (genotype 1b) [8, 15] replicons with respect to cellular growth, HCV RNA titer of replicons in culture and sensitivity to interferon (IFN).

## Materials and Methods

*Cell Culture System and IFN*

Huh7 cells were cultured and maintained in conditions described previously [12]. Recombinant human IFN-$\alpha_{2a}$ (Roferon-A) was obtained from Nippon Roche, Tokyo, Japan.

*Constructs of Subgenomic HCV Replicons*

The construct of a subgenomic HCV replicon of genotype 1b, pFK-$I_{389}$neo/NS3-3′/NK5.1 (pFK/Con1 NK5.1) [8, 15], was a generous gift from Dr. Ralf Bartenschlager (University of Heidelberg, Heidelberg, Germany). The construct of a subgenomic HCV clone of genotype 2a, pSGR-JFH1 (accession number AB114136), was prepared using the JFH-1 strain isolated from a patient with fulminant hepatitis [12].

*RNA Synthesis*

pFK/Con1 NK5.1 was linearized by treatment with *ScaI*. pSGR-JFH1 was digested with *XbaI* and then treated with a mung bean nuclease (New England Biolabs, Beverly, Mass., USA) as described elsewhere [12]. Linearized plasmid DNAs were purified and used as templates for RNA synthesis. Subgenomic HCV RNA was synthesized in vitro with the use of a MEGAscript™ T7 kit (Ambion, Austin, Tex., USA). Synthesized RNA was treated with DNase I (RQ1™ RNase-free DNase, Promega, Madison, Wisc., USA) and extracted with acid phenol to remove any remaining template DNA.

*Transfection with RNA*

Synthesized replicon RNAs were transfected into Huh7 cells by electroporation as described [12]. Briefly, synthesized RNA (0.1 ng to 1 μg) was mixed with suspension of trypsinized Huh7 cells (400 μl; 7.5 × $10^6$ cells/ml). Cells were then pulsed at 260 V and 950 μF in a Gene Pulser II™ apparatus (Bio-Rad, Hercules, Calif., USA). Transfected cells were immediately transferred to culture dishes of 10 cm in diameter, each containing 8 ml of culture medium. G418 (Nacalai Tesque, Kyoto, Japan) in a concentration of 1.0 mg/ml was added to culture medium at 16–24 h after transfection. Culture medium supplemented with G418 was replaced twice weekly. Three weeks after the transfection, cells were fixed with buffered formalin and stained with crystal violet, and some grown colonies were cloned.

*Isolation and Analysis of G418-Resistant Cells*

G418-resistant colonies were independently isolated using a cloning cylinder (Asahi Techno Glass Co., Tokyo, Japan) and cultured until approximately 90% confluence in 10-cm dishes (Corning Inc., N.Y., USA). Total RNA was isolated from cells using the Isogen reagent (Nippon Gene, Tokyo, Japan). Isolated clones and parental Huh7 cell were seeded at 1 × $10^5$ cells/well in 6-well plates (Corning Inc.). In some experiments, replicon cells were seeded at 2 × $10^5$ cells/well in 6-well plates. Cells were harvested daily for determining cell growth and HCV RNA titers. At 24 h after G418 had been removed from the culture medium, serial dilutions of IFN-α (Nippon Roche) were added to wells, and cells were harvested after culture for 72 h.

*Northern Blot Analysis*

Isolated RNA (2.5 or 4 μg) was separated by electrophoresis on 1% (weight/vol) agarose gel containing formaldehyde, then transferred to a positively charged nylon membrane (Hybond-N+, Amersham Pharmacia, Bucks., UK) and immobilized with the use of the Stratalinker UV cross linker (Stratagene, La Jolla, Calif., USA). Hybridization was performed using a DNA probe labeled with [α-$^{32}$P]dCTP in Rapid-Hyb buffer (Amersham Pharmacia). The DNA probe was deduced from *neo*$^r$ and encephalomyocarditits virus internal ribosome entry site genes and synthesized in the Megaprime DNA labeling system (Amersham Pharmacia).

*Quantification of HCV RNA by Real-Time Reverse Transcription Polymerase Chain Reaction*

Copy numbers of HCV RNA were determined by the real-time detection reverse transcription polymerase chain reaction (RTD-PCR) described previously [16] in the ABI Prisom 7700 sequence detector system (Applied Biosystems Japan, Tokyo, Japan). Data were standardized by the concentration of intracellular glyceraldehyde-3-phosphate dehydrogenase.

*Statistics*

Statistical analysis was performed by Student's t test, Welch's t test or the Mann-Whitney U test. Differences with a p value $<0.05$ were considered statistically significant.

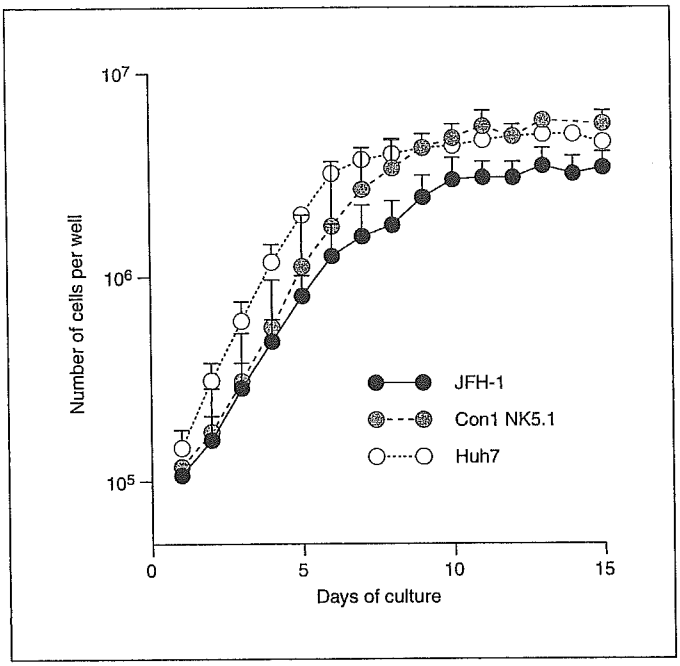


**Fig. 1.** Rate of cell growth. JFH-1 replicon clones, Con1 NK5.1 replicon clones and Huh7 cells were grown in 6-well culture plates and counted daily. Results are expressed by the mean ± SD cell number/well.

**Table 1.** HCV RNA copies detected in isolated clones carrying HCV replicon

| Replicon clone | Number of isolated clones | HCV RNA copies/μg, RNA[a] |
|---|---|---|
| JFH-1 | 19 | $2.73 \pm 2.16 \times 10^7$ |
| Con1 NK5.1 | 6 | $2.38 \pm 2.04 \times 10^7$ |

[a] Mean ± SD.

**Table 2.** Growth rates and cell densities (mean ± SD) of Huh7 and other cell lines harboring HCV replicon

| Cell line | Mean doubling time, h | Saturation density $\times 10^5$ cells/cm$^2$ |
|---|---|---|
| Huh7 | 27.4 ± 3.5[b] | 5.17 ± 0.33[c] |
| JFH-1[a] | 31.2 ± 2.7 | 3.41 ± 0.48 |
| Con1 NK5.1[a] | 28.9 ± 2.9 | 5.56 ± 0.34[c] |

[a] Ten clones of the JFH-1 replicon and 4 clones of Con1 NK5.1 were used in this experiment.
[b] $p < 0.05$ versus JFH-1.
[c] $p < 0.001$ versus JFH-1.

## Results

*Replication of HCV RNA in Clones Transfected with JFH-1 or Con1 NK5.1 Subgenomic HCV RNA*

To determine the replicative ability of the JFH-1 clone, synthetic RNA transcribed from linearized pSGR-JFH1 or pFK/Con1 NK5.1 was transfected into Huh7 cells by electroporation, as described previously [12]. Cells transfected with the Con1 NK5.1 replicon became confluent more rapidly than those transfected with the JFH-1 replicon, until they started to die because of G418; transfected cells were cultured for 3 weeks in the presence of 1 mg/ml G418. Efficiencies of colony formation were 53,200 and 909 colony forming units/μg RNA for JFH-1 and Con1 NK5.1 replicons, respectively [12].

A total of 19 clones were isolated for the JFH-1 replicon and 6 clones for the Con1 NK5.1 replicon. Each clone had been cultured until approximately 80–90% confluence was achieved on the culture dish, whereupon it was harvested. Total RNA was extracted from each replicon clone, and the replication of RNA was confirmed using Northern blot analysis (data not shown). Mean replication levels of HCV RNA determined by RTD-PCR were similar for both replicon clones, $2.73 \pm 2.16 \times 10^7$ copies/μg RNA for JFH-1 and $2.38 \pm 2.04 \times 10^7$ copies/μg RNA for Con1 NK5.1 (table 1). Expressions of HCV proteins were confirmed in all replicon clones by Western blot and immunofluorescence assay (data not shown).

*Growth Curves of Replicon Cells*

Rates of cellular growth were determined on parental Huh7 cells, 10 cloned cells harboring JFH-1 replicon and 4 cloned cells supporting Con1 NK5.1. Each cell line was seeded at $1.0 \times 10^5$ cells/well in 6-well plates, harvested daily and counted. Figure 1 depicts mean rates of cell growth for the JFH-1 replicon, the Con1 NK5.1 replicon and Huh7 cells. The mean doubling time during the logarithmic growing phase was 31.2 ± 2.7 h for JFH-1, 28.9 ± 2.9 h for Con1 NK5.1 and 27.4 ± 3.5 h for Huh7 (JFH-1 vs. Huh7, $p < 0.05$) (table 2). Saturation densities determined by cell counts after they had reached the confluence were $3.41 \pm 0.48 \times 10^5$ cells/cm$^2$ for JFH-1, $5.56 \pm 0.34\ 010^5$ cells/cm$^2$ for Con1 NK5.1 and $5.17 \pm 0.33 \times 10^5$ cells/cm$^2$ for Huh7 (JFH-1 vs. Con1 NK5.1 or Huh7, $p < 0.001$) (table 2). Thus, JFH-1 replicon cells had slower cell growth and lower cell density than parental Huh7 cells.

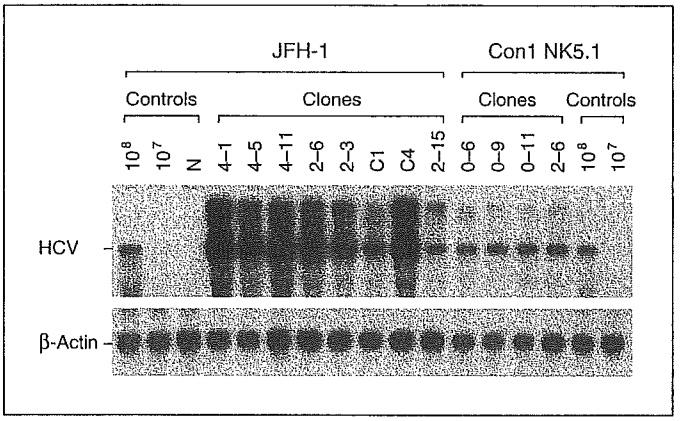


**Fig. 2.** Northern blot analysis of replicon RNA 1 day after the cell passage. Total cellular RNAs (2.5 μg) isolated from JFH-1 and Con1 NK5.1 replicon cells at the next day of passage were loaded onto agarose gel. After electrophoresis, RNAs of HCV or β-actin were detected by the Northern blot with random-primed DNA probes specific to encephalomyocarditits virus internal ribosome entry site and *neo*$^r$ or β-actin sequences, respectively.

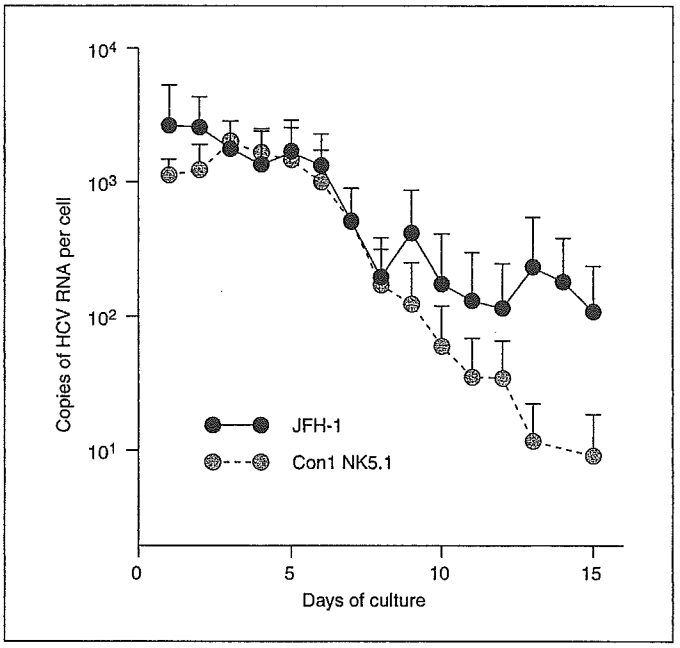


**Fig. 3.** Replication levels of HCV RNA during cell growth. HCV RNA replicating in JFH-1 or Con1 NK5.1 replicon cells were determined by the quantitative RTD-PCR.

Pietschmann et al. [17] reported that the replication level of the Con1 NK5.1 replicon is inversely related to cell growth. Therefore, we compared the number of HCV RNA copies determined by RTD-PCR between JFH-1 and Con1 NK5.1 replicon clones that had been examined for the cell growth. Mean titers of HCV RNA at 1 day after seeding were 2.65 ± 2.36 × $10^3$ copies/cell for JFH-1 and 1.14 ± 0.28 × $10^3$ copies/cell for Con1 NK5.1 ($p = 0.396$). However, most JFH-1 replicon clones emitted HCV RNA signals stronger than those of Con1 NK5.1 replicon clones in Northern blot analysis (fig. 2). HCV RNA levels of both JFH-1 and Con1 NK5.1 replicon cells decreased gradually and became comparable during days 3–8 (fig. 3). Both replicon cells became confluent around day 7–9. However, the mean RNA titer of JFH-1 clones remained around 100 copies/cell, while that of Con1 clones decreased to some 10 copies/cell during days 9–15. When all replicon cells were expanded after cloning, they were 80–90% confluent with HCV RNA titers comparable between JFH-1 and Con1 NK5.1 (table 1). The mean levels of replicon RNA at day 15 were 9.84 ± 12.58 × $10^1$ copies/cell for JFH-1 and 0.93 ± 0.86 × $10^1$ copies/cell for Con1 NK5.1 ($p = 0.0897$). During this experiment, culture medium was replaced on days 4, 8 and 12. The mean level of replicon RNA in JFH-1 clones increased the day after replacement of culture medium. However, RNA levels of Con1 NK5.1 clones were not affected by the replacement of culture medium.

*Effects of IFN on the Replication of Subgenomic RNA*

HCV replicon clones of genotype 1b are reportedly sensitive to IFN-α [10, 18]. However, in the clinical setting, HCV genotype 1b is generally considered resistant to IFN-α, in contrast to HCV genotype 2a which is more sensitive to it. To compare sensitivities of JFH-1 and Con1 NK5.1 replicons to IFN, serially diluted IFN-α was added to cultures of these replicons. After cultivation for 72 h, replicon cells were harvested and cellular RNA was extracted from each culture. RNAs isolated from cloned replicon cells, JFH-1/4–1 and Con1 NK5.1/0–11, were subjected to Northern blot analysis (fig. 4). The copy number of replicon RNA was also determined by RTD-PCR. IFN-α at a concentration of 10 U/ml clearly reduced the replication of Con1 NK5.1/0-11 replicon RNA, whereas JFH-1/4-1 replicon RNA did not decrease with 10 U/ml IFN-α (fig. 4). Copy numbers of HCV RNA were determined by RTD-PCR in 4 clones each for JFH-1 and Con1 NK5.1 replicons. Changes in the copy number of HCV RNA are expressed by the percentage of that cultured without IFN-α shown in figure 5. Inhibitory concentration of 50% ($IC_{50}$) thus calculated was 30.61 ± 15.19 U/ml for JFH-1 replicons and 2.94 ± 1.59 U/ml for Con1 NK5.1 replicons ($p < 0.05$). Although there is a

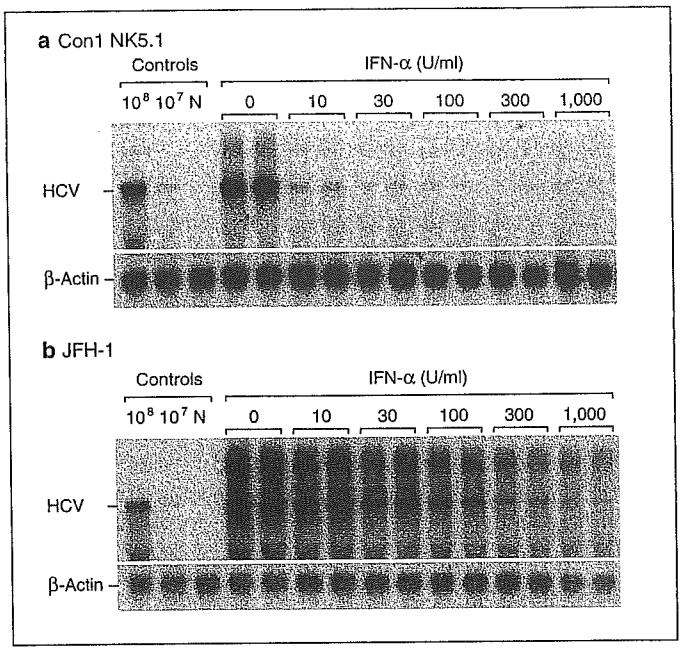


**Fig. 4.** Northern blot analysis of HCV RNAs in Con1 NK5.1/0-11 (**a**) and JFH-1/4-1 (**b**) replicon clones having undergone treatment with IFN-α. Cells were cultured for 72 h in the absence (lanes 4–5) or presence (lanes 6–15) of 10–1,000 U/ml IFN-α.

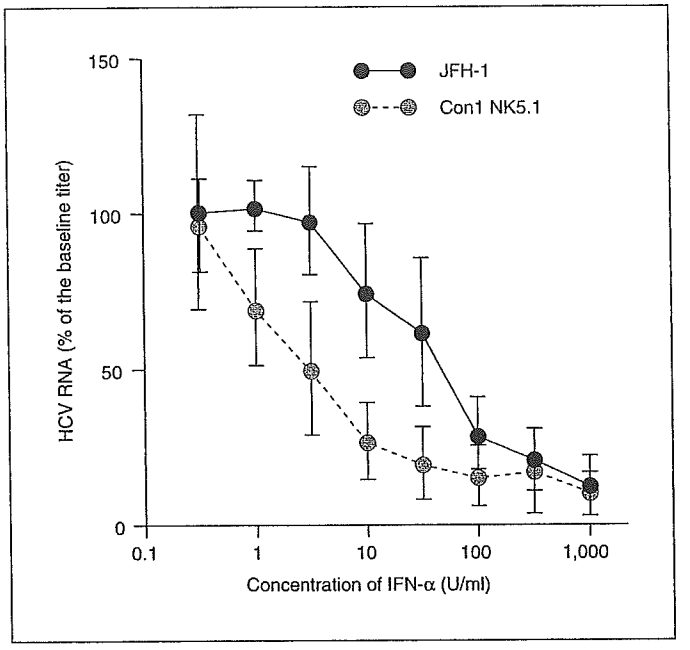


**Fig. 5.** Inhibition of HCV replicons by IFN-α. Four clones each of JFH-1 and Con1 NK5.1 replicons were cultured for 72 h in the absence or presence of 0.3–1,000 U/ml IFN-α. HCV RNA titers in replicon cells were determined by the quantitative RTD-PCR. HCV RNA levels from control cells (without IFN) were set at 100%. The percentage of HCV RNA levels of the JFH-1 or Con1 NK5.1 replicon was calculated and plotted against the concentration of IFN-α. Data were normalized based on the concentration of an internal control (glyceraldehyde-3-phosphate dehydrogenase).

significant difference in $IC_{50}$ between replicons of genotypes 1b and 2a, the mean copy number of HCV RNA extracted from cells in the absence of IFN was different, namely $5.77 \pm 3.7 \times 10^7$ copies/μg RNA for JFH-1 and $5.56 \pm 6.21 \times 10^6$ copies/μg RNA for Con1 NK5.1. Thus, the difference in $IC_{50}$ between genotypes may be due to different replication capacities of the clones tested rather than a distinct response to IFN-α.

## Discussion

Since the discovery of HCV, numerous sequences of HCV isolates have been reported. Comparison of these sequences has highlighted a marked genetic heterogeneity of the HCV genome, by which HCV isolates have been classified into six genotypes. Among them, genotypes 1 and 2 are distributed worldwide [6]. Increasing lines of evidence indicate that patients infected with HCV of different genotypes may present with distinct clinical profiles, in terms of severity of liver disease and response to antiviral therapies [7]. For example, genotype 1b is known to be resistant to IFN, whereas genotype 2a is sensitive to it. However, because of its ubiquity, investigations of viral characteristics have been mostly conducted on HCV isolates of genotype 1b. The newly established subgenomic replicon of genotype 2a [12] has provided opportunities for evaluating differences in viral characteristics between genotypes 1 and 2 to improve our understanding on mechanisms of viral replication and persistence.

In this study, we compared subgenomic HCV replicons of genotype 1b with genotype 2a, using Con1 NK5.1and JFH-1 strains, respectively. As reported previously [12], the efficiency of colony formation is higher for JFH-1 than for Con1 NK5.1. However, HCV RNA titers of both replicons did not differ when harvested after cloning procedures (table 1). The efficiency in colony formation may reflect the replication capacity of the original HCV strain rather than HCV RNA titers of replicon cells, since levels of HCV RNA replication in the selected clones may have been enhanced through G418 selection and cloning procedure. However, a high replication efficiency of the JFH-1 replicon has been demonstrated in a transient replication of JFH-1 in Huh7 cells in the ab-